Secondary organic aerosol reduced by mixture of atmospheric vapours

Gordon McFiggans[1], Thomas F. Mentel[2], Jürgen Wildt[2,3], Iida Pullinen[2,15], Sungah Kang[2], Einhard Kleist[3], Sebastian Schmitt[2,16], Monika Springer[2], Ralf Tillmann[2], Cheng Wu[2,17], Defeng Zhao[5,2], Mattias Hallquist[6], Cameron Faxon[6], Michael Le Breton[1,6], Åsa M. Hallquist[7], David Simpson[8,12], Robert Bergström[6,8,13], Michael E. Jenkin[9], Mikael Ehn[10], Joel A. Thornton[11], M. Rami Alfarra[1,14], Thomas J. Bannan[1], Carl J. Percival[1,18], Michael Priestley[1], David Topping[1,14], Astrid Kiendler-Scharr[2,4]

1. University of Manchester, School of Earth and Environmental Sciences, Oxford Road, Manchester, M13 9PL, UK
2. Institut für Energie- und Klimaforschung, IEK-8, Forschungszentrum Jülich, 52425 Jülich, Germany
3. Institut for Bio- and Geosciences, IBG-2, Forschungszentrum Jülich, Jülich 52425, Germany
4. I. Physikalisches Institut, Universität zu Köln, 50937 Köln, Germany
5. Department of Atmospheric and Oceanic Sciences & Institute of Atmospheric Sciences, Fudan University, Shanghai, China
6. Atmospheric Science, Department of Chemistry and Molecular Biology, University of Gothenburg, SE-41296 Gothenburg, Sweden
7. IVL Swedish Environmental Research Institute, PO Box 5302, SE-400 14 Gothenburg, Sweden
8. Department of Earth, Space and Environment, Chalmers University of Technology, 41296 Gothenburg, Sweden
9. Atmospheric Chemistry Services, Okehampton, Devon, EX20 4QB, UK
10. Institute for Atmospheric and Earth System Research / Physics, Faculty of Science, University of Helsinki, P.O. Box 64, 00014, Helsinki, Finland
11. Department of Atmospheric Sciences, University of Washington, Seattle, WA98195, USA
12. EMEP MSC-W, Norwegian Meteorological Institute, Oslo, Norway
13. Swedish Meteorological and Hydrological Institute, 60176 Norrköping, Sweden
14. National Centre for Atmospheric Science (NCAS), Oxford Road, Manchester, M13 9PL, UK
15. Department of Applied Physics, University of Eastern Finland, 70211 Kuopio, Finland
16. TSI GmbH, 52068 Aachen, Germany
17. Stockholm University, Department of Environmental Science & Analytic Chemistry, SE-10691 Stockholm, Sweden
18. Jet Propulsion Laboratory, California Institute of Technology, Pasadena, CA 91109, USA

Secondary organic aerosol contributes to the atmospheric particle burden with implications for air quality and climate. Biogenic volatile organic compounds emitted from plants are important secondary organic aerosol precursors with isoprene emissions dominating globally. However, its yield of particle mass from oxidation is generally modest compared to that of other terpenoids. Here we show that isoprene, carbon monoxide and methane can suppress the instantaneous mass and the overall mass yield derived from monoterpenes in mixtures. We find that isoprene scavenges hydroxyl radicals preventing reaction with monoterpenes and the resulting isoprene peroxy radicals scavenge highly oxygenated monoterpene products. These effects reduced the yield of low-volatility products that would otherwise form secondary organic aerosol. Global model calculations indicate that oxidant and product scavenging can operate effectively in the real atmosphere. Highly reactive, modest aerosol yield compounds are not necessarily net producers and their oxidation can suppress both particle number and mass.

Introduction

The secondary organic fraction of fine aerosol is substantial[1,2] and contributes significantly to the fine particulate matter (PM) burden[3] and aerosol impacts on climate[4]. Conventionally, Secondary Organic Aerosol (SOA) particle mass is considered to be formed independently from the condensable oxidation products of each contributing volatile organic compound (VOC)[5]. The ambient atmosphere is a complex mixture of biogenic and anthropogenic VOC, a limited number of which are normally considered to control the oxidant concentrations in air quality or climate models[4,5]. Isoprene has been found to dominate plant VOC emissions globally[6,7], though it has been found only moderately effective at forming SOA particle mass[8,9,10]. Nevertheless, isoprene oxidation tracers have been observed in particles in both chamber experiments[11,12] and the atmosphere[11,13,14,15] showing that they condense from the gas phase. Oxidation of the monoterpenes (MT), including α-pinene, and sesquiterpenes is generally more efficient at producing SOA particle mass[16,17,18]. When oxidation of a VOC contributing to SOA is explicitly considered in models, some interaction between the oxidant field and the SOA formation process is implicit[5], though recently observed behaviour is yet to be described. Two such recent findings have motivated the current work. First, it has been shown that C_5 isoprene molecules suppress the nucleation of SOA particles in the oxidation of the C_{10} MT in mixtures of plant emissions by successfully competing for the hydroxyl radical, OH[19,20,21]. Second, recent direct observation of highly oxygenated organic molecules (HOM) formed from MT oxidation[22], and elucidation of the auto-oxidation mechanisms by which they are formed, have implicated them in the formation of new SOA particles. Our work moves beyond the suppression of particle nucleation by isoprene using the new mechanistic understanding to explain SOA mass and yield suppression in MT-containing mixtures. These results highlight a need for more realistic consideration of SOA formation in the atmosphere analogous to the treatment of ozone formation, where interactions between the mechanistic pathways involving peroxy radicals are recognised to be essential[23].

Use of SOA yields in mixtures

Ostensibly, the concept of a SOA yield is straightforward and unambiguous[24-26]. It has been widely used to interpret the potential of precursor molecules to produce particulate mass, most extensively from smog chamber studies and usually with the goal of quantifying the formation of ambient atmospheric particles. Yield is normally defined in terms of the particulate mass condensed for a given mass of gaseous parent VOC consumed. The process of determining SOA yields presents substantial practical challenges. Notwithstanding measurement uncertainties and artefacts (for example, wall losses and those associated with the accurate determination of the mass of semi-volatile material[27-31]) there are numerous reasons why SOA yields may vary according to the conditions under which they are measured. This paper does not aim to provide a critical evaluation of the determination of SOA yields and their extrapolation to atmospheric conditions and the reader is referred to a number of recent publications for a discussion of challenges and the state-of-the-science concerning the interpretation of SOA formation from chamber experiments[22,27,29-32]. However, there are conceptual aspects often implicit in the treatment of SOA formation either in chamber experiments, real atmospheric mixtures, or models of the atmosphere that provide the context for the current study.

First, the concept of yield frequently includes some assumption of equilibrium. An interpretation of particle mass in terms of the partitioning of components of known volatility by absorptive partitioning invokes an equilibrium assumption. In reality, mass takes a finite time to transfer between the continuous and dispersed phases[33,34]. Second, a parent VOC will continue to react, as will its reaction products, provided they have reaction partners. Under atmospheric, or simulated atmospheric, conditions the reaction partners are normally oxidants, such as the hydroxyl radical OH (the main focus in this paper). This means that the distribution of vapour phase components that is available to transfer to the condensed phase by condensational growth or nucleation is continuously evolving through photochemical reactions. Third, a yield integrates across all oxidation products formed from the parent hydrocarbon, summing the fraction of these products that will partition to the particle phase from whatever stage of oxidation under the chosen reaction conditions. We further would like to note that the yields themselves can be dependent on the oxidant concentration[e.g.31,32].

This combination of characteristics raises first order challenges when considering SOA formation in the real atmosphere which comprises a complex mixture of organic vapours of widely varying volatilities, from numerous sources of anthropogenic and biogenic origin. This paper is concerned with the challenge surrounding the introduction of oxidants into the atmospheric mixture and the reactivity of the evolving components in the mixture – specifically, the yield of condensed organic particulate material of any of the single component vapours in the mixture when it is consumed by the oxidant. Any of the vapours may react with the available oxidant, so from the perspective of any other vapour molecule, the oxidant has been "scavenged" and is unavailable as a reaction partner. Our experimental systems illustrate the implications on SOA formation of mixtures of precursors. We demonstrate how SOA yield in mixtures is dependent on whether the reactivity of one of the SOA forming compounds controls the oxidant and contrast conditions in the laboratory and the atmosphere. It is not only the oxidants that can be removed from the system by components of a mixture. The products from oxidation that can react to form the final condensable SOA precursors may alternatively be scavenged by other reactive intermediates. This process can form the basis for the reduction in yield of the individual components in a mixture, as shown by our results below and detailed in the supplement sections.

Experiments to SOA formation in mixtures

In the Jülich Plant Atmosphere Chamber (JPAC; suppl. section 1) we find that the presence of isoprene substantially suppresses the SOA mass formed from oxidation of α-pinene, the most abundant MT in the atmosphere (Figure 1A). Furthermore, we show that this reduction of SOA mass is not trivially due to the lower amount of MT consumed in the presence of isoprene. Rather the presence of isoprene actually suppresses the SOA mass yield from the amount of VOC consumed (Figure 1B). Isoprene thereby limits not only new particle formation[19] (hence exhibiting control over particle number concentration) but also the growth of pre-existing particles and thus their size. This has significant consequences for the abundance of PM mass formed in the mixture and the number of particles that may grow to sizes where they can act as cloud seeds. Our findings are surprising and unexpected in the context of existing conceptions of SOA mass yields (suppl. section 2). As shown in Figure 1, the presence of isoprene substantially suppresses the SOA mass formation from α-pinene oxidation by about 60% and the SOA yield by 40%. Figure S2 shows even greater suppression in greater isoprene excess, with both mass and yield reduced in the presence of both neutral and acidic seed. This contrasts sharply with current understanding, since isoprene oxidation should contribute substantially to SOA production when isoprene concentrations are high.

Below we describe the two effects contributing to SOA suppression - oxidant scavenging and product scavenging. This demonstrates the importance of accounting for the reactivity of the parent VOC in atmospheric mixtures and hence their turnover (suppl. section 2) as well as interactions between their reaction intermediates and products. Whilst our experiments illustrate this requirement predominantly with reference to the photochemical isoprene – α-pinene system with OH as the major oxidant, it should be noted that in all mixed systems investigated, OH (oxidant) scavenging and product scavenging were found to reduce both the SOA particle mass and the SOA yield. Note that during daytime, both, ozonolysis and OH oxidation of α-pinene, contribute to SOA, as in our experiments, however the contribution via OH reactions here was much greater than 90%. According to our mechanistic understanding presented below, product scavenging will be similarly effective for OH and O_3 oxidation.

Oxidant and product scavenging

Oxidant scavenging is demonstrated by the decrease in SOA mass and yield of the mixture with increasing isoprene fraction as well as by the decrease of the α-pinene yield itself (Figure 1B and suppl. section 3). The contribution of isoprene to SOA mass in the presence of neutral ammonium sulfate aerosols is small and α-pinene oxidation products make up the overwhelming fraction of SOA in mixtures. Isoprene increasingly efficiently competes with α-pinene for the available OH as the reaction system is stepped from high SOA yield pure α-pinene to low SOA yield pure isoprene (Figure S2). With respect to α-pinene, the isoprene "scavenges" the OH[19], i.e. the steady state OH concentration is lowered by the introduction of isoprene for a given OH source strength, therefore less OH can react with α-pinene, resulting in less SOA mass being formed. In addition, the SOA yield itself is dependent on [OH][31,32].

By uniquely being able to control the OH at the same concentration with and without isoprene addition by readjusting its source strength, we were able to reveal that the SOA

mass (Figure 1A), and by implication the α-pinene SOA yield (Figure 1B, 3rd bar), decreased with increasing isoprene in the mixture (suppl. section 4). Strikingly, the α-pinene SOA yield was reduced by 30% relative to the pure α-pinene yield, even though the OH scavenging effect has been removed (Δisoprene/Δα-pinene≈1±0.2 [ppb/ppb] = 0.5±0.1 [μg/μg]). Moreover, by re-adjusting [OH], we held the α-pinene sub-system of the mixture at the same stage of oxidation as in the pure case. This results in the condensing oxidation products having the same "chemical age" in both cases, thereby avoiding comparison of chemical systems of different chemical evolution.

In Figure 2 we show the actual α-pinene SOA yields (y_{act}) in the mixture normalized to the α-pinene SOA yield y_{AP} = 17% for pure α-pinene in absence of isoprene. The y_{act} were calculated from the observed SOA mass and the actual consumption of α-pinene. Depending on the isoprene to α-pinene ratio, SOA mass produced from the same amount of consumed α-pinene in the presence of isoprene can be reduced by more than half compared to the amount formed when oxidised alone (Figure 2). Clearly, smaller amounts of SOA forming products from α-pinene oxidation are formed in the presence of isoprene – we denote this effect "product scavenging" .

The product scavenging effect (and the OH scavenging effect) on SOA formation is somewhat masked in the presence of the acidic seed aerosol with which isoprene has a significant yield[12,35-37] (suppl. section 4, Figure S3, Figure 1B, 6th bar). Replacing isoprene by CO shows, that the acidity of the seed particles did not affect the behaviour of α-pinene (Figure S3), but indeed enhanced the isoprene contribution (Figure S4). This underlines the importance of liquid phase processes for isoprene, but also clearly shows that both scavenging effects are general phenomena in the gas phase.

SOA yield suppression also occurs when isoprene is mixed with β-pinene and when CO or CH_4 were mixed with α-pinene (suppl. section 5, Figures S5-S7, Figure 4). This generality ensures that the influence of the relative reactivity of components in mixtures on the SOA formation potential has much more profound implications than a simple reduction in yield in each of the binary mixtures. Moreover, because of potential interactions with additional SOA contributors, the yields in anything beyond the binary mixtures cannot be simply added or in any way predicted without specific mechanistic insight.

The key to a mechanistic understanding of the product scavenging is the formation of HOM with the peculiarity that HOM peroxy radicals also dimerise in the gas phase[38] (suppl. section 6). It can be inferred from their structure and O/C ratios that HOM and even moreso their dimers, are low to extremely low volatility organic compounds[22,39] and will contribute substantially to SOA formation and initial growth[22,39].

In Figure 3A we present direct observation of the product scavenging of α-pinene HOM by comparing mass spectra measured in OH reaction systems for α-pinene-only and for an α-pinene/isoprene mixture. For α-pinene-only we observed about equal signal intensities in the ranges of α-pinene HOM monomers with 10 C-atoms and of HOM dimers with 17-20 C-atoms. In the presence of isoprene, α-pinene dimers are suppressed by a factor of about 3. Comparable dimer suppression by a factor of 2 is observed for CO **(**Figure 4A). HOM dimers have been observed in the boreal ambient atmosphere, lower during daytime than at night-time, but at lower fractions than in our α-pinene-only experiments[40,41]. Since product scavenging will be occurring, particularly during daytime, these observations are consistent with our findings.

The strength of product scavenging is estimated by comparing two sets of experiments where the [OH] was tuned, either by varying the OH sink through adding different amounts of isoprene to the reaction system or by varying the OH production rate through modifying the photolysis rate $J(O^1D)$ for O_3 (Figure 3B). With increasing

isoprene, the dimers are more strongly suppressed than with decreasing $J(O^1D)$ as a result of increased scavenging of α-pinene HOM peroxy radicals by isoprene related RO_2 and HO_2 radicals[42]. This leads to formation of less HOM, mainly by diminishing α-pinene HOM self-dimerization. Suppression of the HOM dimers alone accounts for 27% reduction in HOM mass (Figure 3C) and explains most of the 35% SOA mass reduction by the product scavenging effect shown in Figure 1, underlining the pivotal role of HOM dimers in new particle and SOA formation[22,39]. The involvement of HOM does not preclude the involvement of multigenerational oxidation as such (cf. suppl. section 6). Indeed, the non-linear dependence of the total HOM on the turnover in Figure 3B requires at least a second oxidation step and explains the dependence of the α-pinene SOA yield on [OH], contributing to the OH scavenging effect.

The mechanism of product scavenging via dimer suppression by short chained peroxy radicals or HO_2 is general for peroxy radical chemistry and is not limited to the presence of isoprene in the mixture. It is effective in mixtures of α-pinene with CO via HO_2 (Figure 4) and with CH_4 via CH_3O_2 radicals (Figures S7). CO and CH_4 are extreme cases, each with essentially no SOA yield. In both cases, the scavenging effects are solely related to gas-phase chemistry and independent of aerosol composition: organic or inorganic neutral or inorganic acidic particles. We therefore conclude that product scavenging effect is a general effect in mixtures of VOC.

Atmospheric implications

Our new findings in JPAC would hold in atmospheric concentration regimes (suppl. section 7). However, in the atmosphere, the OH concentration is not solely controlled by the isoprene / α-pinene ratio as in the JPAC chamber. Simulations using the EMEP MSC-W model[43,44] (suppl. section 8) show that the scavenging effects by isoprene under realistic atmospheric conditions lowers the OH concentration compared to the hypothetical "no isoprene" case and affects the SOA formation. However, even at small isoprene SOA yields, the gains of isoprene SOA and MT-O_3-SOA offset the reduction from OH scavenging (Figure 5, noIso, OHS). When a parameterisation of the product scavenging constrained to our measurements (Figure 2) is included in the global model simulations, we find that photochemically generated MT-OH-SOA is strongly suppressed, in areas with sufficiently high MT and isoprene emissions (Figure 5, PS). The dramatic effects on MT-OH-SOA show the potential for product scavenging to reduce aerosol loadings substantially in many regions of the world, even more so if one considers that product scavenging similarly could also affect e.g. the MT-O_3-SOA (Figure 5, PSox). It is not possible to be so sure about the magnitude of OH scavenging from all potential reactants, since more measurement constraint is needed to include mechanistic descriptions in such systems.

Extending our results from mixtures of isoprene, CH_4, and CO with α-pinene or β-pinene to the reactive atmospheric mixture of vapours, any of the reaction products from any of the components in the mixture may react together, such that from the perspective of any of the others, they have been “scavenged” from the mixture. Similarly, from the perspective of the formation of organic particulate material, some of the condensable oxidation products that are direct precursors may be “scavenged”, in all cases reducing the ambient yield. Spatial distribution of short chain organic compounds and specific composition of the reaction mixture will determine the strength of the OH and the product scavenging effects. Whilst long lived compounds, like CH_4, may act ubiquitously in cleaner regions of the earth, compounds with strong anthropogenic sources, like CO, may not exert their full scavenging potential because, when high in concentration, they are always accompanied by high concentrations of

other pollutants, like NO_X. While oxidant scavenging will take place under nearly all conditions, product scavenging across SOA precursors is a complex function RO_2-terminating agents, such as peroxy radicals of VOC with moderate or no SOA yield, HO_2, and NO_X. Product scavenging and "non-additivity" of SOA yields will thus vary from region to region, accordingly. Without further experimentally constrained parameterisation of the interactions between all relevant components in realistic atmosphere, it is not possible to predict the magnitude and geographical distribution of suppression of SOA formation. Inclusion of explicit interactions of such complexity in global simulations is practically impossible. It is only possible to say for the considered systems that the SOA yields and net SOA mass must be reduced compared to linear addition of yields, even if the control of oxidant were realistically included.

Outlook and recommendations

Our findings demonstrate that SOA precursors with modest yields suppress SOA forming products of higher SOA yield precursors substantially. Our work directly challenges two widespread treatments of SOA formation and suggests an alternative mechanistically-based solution. A first obvious recommendation following this work is that the decoupling of the modulation of oxidant fields from SOA precursor turnover is clearly discouraged. We have further demonstrated that simple linear addition of SOA mass from the individual yields of components in a VOC mixture will likely lead to a substantial overestimation of SOA production. Measuring SOA yields with individual compounds leads to insight into the mechanisms of SOA production but the results do not reflect the conditions of the real environment. Such data should therefore be used with caution when modelling aerosol formation. In the general case, the abundance of HOM, HOM-RO_2 and RO_2 products from potential SOA precursors as well as from volatile compounds not producing SOA mass should be considered when predicting the mixture's yield. Our results highlight a need for more realistic consideration of SOA formation in the atmosphere analogous to the treatment of ozone formation, where interactions between the mechanistic pathways involving peroxy radicals are recognised to be essential[23]. It may be possible to produce lumped classes of precursors according to their likelihood of increasing or decreasing a mixture's yield and this could be a focus of further investigation.

It is likely that both background oxidant concentrations and VOC emissions (and hence OH reactivity) will change in the future. Without a reasonable representation of SOA yields in different atmospheric VOC mixtures it will not be possible to achieve predictive capability for the SOA contribution to particulate matter.

References

1. Hallquist, M. *et al.* The formation, properties and impact of secondary organic aerosol: current and emerging issues. *Atmos. Chem. Phys.* **9**, 5155-5236 (2009).

2. Jimenez, J. L. *et al.* Evolution of Organic Aerosols in the Atmosphere. *Science*, **326**, 1525-1529 (2009)

3. Goldstein, A. H. & I. E. Galbally, Known and Unexplored Organic Constituents in the Earth's Atmosphere, *Environ. Sci. & Technol.* **41**, 1514-1521 (2007).

4. Spracklen, D.V. *et al.* Aerosol mass spectrometer constraint on the global secondary organic aerosol budget. *Atmos. Chem. Phys.* **11**, 12109-12136 (2011).

5. Kanakidou, M. *et al.* Organic aerosol and global climate modelling: a review. *Atmos. Chem. Phys.* **5**, 1053-1123 (2005).

6. Guenther, A. *et al.* Estimates of global terrestrial isoprene emissions using MEGAN (Model of Emissions of Gases and Aerosols from Nature). *Atmos. Chem. Phys.* **6**, 3181-3210 (2006).

7. Guenther, A. *et al.* The Model of Emissions of Gases and Aerosols from Nature version 2.1 (MEGAN2.1): an extended and updated framework for modeling biogenic emissions. *Geosci. Model Dev.* **5**, 1471-1492, (2012).

8. Carlton, A.G., Wiedinmyer, C., & Kroll, J.H. A review of Secondary Organic Aerosol (SOA) formation from isoprene. *Atmos. Chem. Phys.* **9**, 4987-5005 (2009).

9. Clark, C.H. *et al.* Temperature Effects on Secondary Organic Aerosol (SOA) from the Dark Ozonolysis and Photo‐Oxidation of Isoprene. *Environ. Sci. & Techn.* **50**, 5564-5571 (2016).

10. Liu, J. *et al.* Efficient Isoprene Secondary Organic Aerosol Formation from a Non‐IEPOX Pathway. *Environ. Sci. & Technol.* **50**, 9872-9880, (2016).

11. Edney, E.O. *et al.* Formation of 2-methyl tetrols and 2-methylglyceric acid in secondary organic aerosol from laboratory irradiated isoprene/NOX/SO2/air mixtures and their detection in ambient PM2.5 samples collected in the eastern United States. *Atmos. Environ.* **39**, 5281–5289 (2005).

12. Surratt, J.D. *et al.* Reactive intermediates revealed in secondary organic aerosol formation from isoprene. *Proc. Natl. Acad. Sci. USA* **107**, 6640-6645 (2010).

13. Claeys, M. *et al.* Formation of secondary organic aerosols from isoprene and its gas-phase oxidation products through reaction with hydrogen peroxide. *Atmos. Environ.* **38**, 4093-4098 (2004).

14. Robinson, N.H. *et al.* Evidence for a significant proportion of Secondary Organic Aerosol from isoprene above a maritime tropical forest. *Atmos. Chem. Phys.* **11**, 1039-1050 (2011).

15. Xu L. *et al.* Effects of anthropogenic emissions on aerosol formation from isoprene and monoterpenes in the southeastern United States. *Proc. Natl. Acad. Sci. USA* **112**, 37-42 (2015).

16. Lee, A. *et al.* Gas-phase products and secondary aerosol yields from the ozonolysis of ten different terpenes, *J. Geophys. Res.* **111**, D07302 (2006).

17. Lee, A., *et al.* Gas-phase products and secondary aerosol yields from the photooxidation of 16 different terpenes, *J. Geophys. Res.* **111**, D17305 (2006).

18. Ng, N. L. *et al.* Effect of NOx level on secondary organic aerosol (SOA) formation from the photooxidation of terpenes. *Atmos. Chem. Phys.* **7**, 5159-5174 (2007).

19. Kiendler-Scharr, A. *et al.* New particle formation in forests inhibited by isoprene emissions. *Nature* **461**, 381-384 (2009).

20. Kanawade, V.P. *et al.* Isoprene suppression of new particle formation in a mixed deciduous forest. *Atmos. Chem. Phys.* **11**, 6013-6027 (2011).

21. Lee, SH *et al.* Isoprene suppression of new particle formation: Potential mechanisms and implications. *J. Geophys. Res. Atmos.* **121**, 14,621-14,635 (2016).

22. Ehn, M. *et al.* A large source of low-volatility secondary organic aerosol. *Nature* **506**, 476–479 (2014).

23. Jenkin, M.E., Derwent, R.G. & Wallington, T.J. Photochemical ozone creation potentials for volatile organic compounds: Rationalization and estimation. *Atmos. Environ.* **163**, 128-137 (2017).

24. Odum, J. R. *et al.* Gas/particle partitioning and secondary organic aerosol yields. *Environ. Sci. & Tech.* **30**, 2580-2585 (1996).

25. Hoffmann, T. *et al.* Formation of organic aerosols from the oxidation of biogenic hydrocarbons. *J. Atmos. Chem.* **26**, 189-222 (1997).

26. Seinfeld, J. H. & Pankow, J. F. Organic atmospheric particulate material. *Ann. Rev. Phys. Chem.* **54**, 121-140 (2003).

27. Matsunaga, A. & Ziemann, P. J. Gas-Wall Partitioning of Organic Compounds in a Teflon Film Chamber and Potential Effects on Reaction Product and Aerosol Yield Measurements. *Aerosol Sci. Tech.* **44**, 881-892 (2010).

28. Zhang, X. *et al.* Influence of vapor wall loss in laboratory chambers on yields of secondary organic aerosol. *Proc. Natl. Acad. Sci. USA* **111**, 5802-5807 (2014).

29. Zhang, X. *et al.* Vapor wall deposition in Teflon chambers. *Atmos. Chem. Phys.* 15, 4197- 4214 (2015).

30. Krechmer, J. E., Pagonis, D., Ziemann, P. J. & Jimenez, J. L. Quantification of Gas-Wall Partitioning in Teflon Environmental Chambers Using Rapid Bursts of Low-Volatility Oxidized Species Generated in Situ. *Environ. Sci. Tech.* **50**, 5757- 5765 (2016).

31. Sarrafzadeh, M. *et al.* Impact of NOx and OH on secondary organic aerosol formation from β-pinene photooxidation. *Atmos. Chem. Phys.* **16**, 11237-11248 (2016).

32. Eddingsaas, N. C. *et al.* Alpha-pinene photooxidation under controlled chemical conditions - Part 2: SOA yield and composition in low- and high-NOx environments. *Atmos. Chem. Phys.* **12**, 7413-7427, (2012).

33. Zhang, X., Pandis, S. N. & Seinfeld, J. H. Diffusion-Limited Versus Quasi-Equilibrium Aerosol Growth. *Aerosol Sci. Tech.* **46**, 874-885 (2012).

34. O'Meara, S., Topping, D. O. & McFiggans, G. The rate of equilibration of viscous aerosol particles. *Atmos. Chem. Phys.* **16**, 5299-5313 (2016).

35. Surratt, J. D. *et al.* Effect of acidity on secondary organic aerosol formation from isoprene. *Environ. Sci. & Techn.* **41**, 5363-5369 (2007).

36. Gaston, C. J. *et al.* Reactive Uptake of an Isoprene-Derived Epoxydiol to Submicron Aerosol Particles. *Environ. Sci. & Techn.* **48**, 11178-11186 (2014).

37. Riva, M. *et al.* Effect of Organic Coatings, Humidity and Aerosol Acidity on Multiphase Chemistry of Isoprene Epoxydiols. *Environ. Sci. & Techn.* **50**, 5580-5588 (2016).

38. Berndt, T. *et al.* Accretion Product Formation from Self- and Cross-Reactions of RO_2 Radicals in the Atmosphere. *Angew. Chem. Int. Edit.* **57**, 3820-3824 (2018).

39. Tröstl, J. *et al.* The role of low-volatility organic compounds in initial particle growth in the atmosphere. *Nature* **533**, 527-531 (2016).

40. Mohr, C. *et al.* Ambient observations of dimers from terpene oxidation in the gas phase: Implications for new particle formation and growth. *Geophys. Res. Lett.* **44**, 2958-2966 (2017).

41. Yan, C. et al. Source characterization of highly oxidized multifunctional compounds in a boreal forest environment using positive matrix factorization. *Atmos. Chem. Phys.* **16**, 12715-12731 (2016).

42. Wennberg, P. O. *et al.* Gas-Phase Reactions of Isoprene and Its Major Oxidation Products. *Chem. Reviews* **118**, 3337-3390 (2018).

43. Simpson, D. *et al.* The EMEP MSC-W chemical transport model - technical description. *Atmos. Chem. Phys.* **12**, 7825-7865 (2012).

44. Stadtler, S. *et al.*, Ozone impacts of gas-aerosol uptake in global chemistry-transport models. *Atmos. Chem. Phys.* **18**, 3147-3171 (2018)

Author contributions:

G.M, T.F.M., J.W. edited the manuscript and the supplement
G.M., T.F.M., J.W., A.K.S., M.H, D.S. M.E.J. conceptualized and planned the study, and conducted data interpretation
J.W. I.P., S.K., E.K., S.S., M.S., R.T., C.W., D.Z., C.F., M.L.B., Å.M.H., M.R.A., T.J.B., C.J.P., M.P., D.T conducted data collection and analysis
D.S., R.B., M.E.J. contributed the global model calculations
J.T., M.E., Å.M.H., M.H. provided specific inputs to manuscript and supplement
All co-authors discussed the results and commented the manuscript and the supplement.

Acknowledgements

This is a pre-print of an article published in Nature. The final authenticated version is available online at: https://doi.org.10.1038/s41586-018-0871-y

The EMEP modelling work has been partially funded by EMEP under UNECE. Computer time for EMEP model runs was supported by the Research Council of Norway through the NOTUR project EMEP (NN2890K) for CPU, and NorStore project European Monitoring and Evaluation Programme (NS9005K) for storage of data. The research presented is a contribution to the Swedish strategic research area ModElling the Regional and Global Earth system, MERGE. This work was supported by Formas (grant numbers 214-2010-1756, 942-2015-1537); the Swedish Research Council (grant number 2014-5332) and the European Research Council (Starting grant no 638703, "COALA"). ÅMH acknowledge Formas (214-2013-1430) and Vinnova, Sweden's Innovation Agency (2013-03058), including support for her research stay at FZJ. Participation of the Manchester group was facilitated by the UK Natural Environment Research Council (NERC) funded CCN-Vol project (NE/L007827/1) and underpinning National Centre for Atmospheric Science (NCAS) funding.

Data availability statements

All data used are shown as Figures or Tables in the manuscript or in the supplemental information. Raw data are available from the corresponding author on reasonable request.

Figure Captions

Figure 1: Reduced *SOA mass* and *yield* of α-pinene by *product scavenging* and *OH scavenging* by isoprene.
The top panel depicts symbolically the transition of the reaction system. **a**: Neutral seed particles: isoprene (red triangles) lowered [OH] (black diamonds) and the corresponding consumption of α-pinene (blue squares), reducing the organic mass dramatically. The organic mass was normalized to sulfate mass (organics/SO_4^{2-}, green circles). The newly discovered product scavenging (red) in the presence of isoprene is separated from OH scavenging (orange) by re-adjustment of [OH]. Because of product scavenging only 60% of the organic mass is formed despite the same α-pinene consumption. (The acidic case is depicted in Figure S3.) Vertical error bars for Δα-pinene and Δisoprene are s.d. for averaging 14-15 samples, horizontal bars show the averaging intervals. For OH we estimate an overall error of ±33%.
b: The SOA yields in presence of neutral ammonium sulfate (blue) and acidic ammonium bisulfate (red) seed particles were calculated at times B, C, and, D as *organic mass*/*α-pinene consumption* (acidic seed particles, see suppl. section 3). Not only the SOA mass (indicated by the green spheres in the middle) but also its yield decreased strongly (bar plots). B shows the SOA yield for α-pinene alone, while C shows the summed effect of the new product scavenging and OH scavenging in the α-pinene & isoprene reaction system. For the neutral seeds D demonstrates the magnitude of the product scavenging effect on the SOA yield, as [OH] and α-pinene consumption were re-adjusted to the same levels as before isoprene addition. On acidic seed aerosol (red) isoprene makes a substantial contribution to SOA, which compensates for some of the OH scavenging effect and most of the product scavenging effect. The errors reflect the estimated overall 15% uncertainty for an individual experiment.

Figure 2: The reduction of the SOA yield of α-pinene by isoprene as a function of the isoprene/α-pinene consumption (Δisoprene/Δα-pinene).
The actual SOA yield of α-pinene (y_{act} = Δorganic mass / Δα-pinene) in α-pinene & isoprene mixtures was normalized to the average SOA yield obtained with α-pinene-only (y_{AP}) at same conditions for neutral (blue) and acidic seeds (red). The grey area indicates the ±20% band for the scattering of the α-pinene-only yields around y_{AP} = 0.17 which includes the 15% error in the individual SOA mass yields (vertical bars) and the variability of the experimental conditions for the reaction system with α-pinene-only. Horizontal error bars show the uncertainties of the isoprene/α-pinene ratio (±10%) derived from the measurement errors of the compounds.
The dashed line is the fit to the results for the neutral seeds that was implemented in the global model calculations to parametrize product scavenging:
$y_{act} = y_{AP} \cdot (0.48+0.52 \cdot \exp[-1.53 \cdot (\Delta isoprene/\Delta \alpha\text{-}pinene)])$

Figure 3: HOM monomer/dimer distribution in the presence and absence of isoprene illustrating the product scavenging effect.
a: comparison of two mass spectra taken in experiments with (orange) and without isoprene (blue). In the presence of isoprene the dimer/monomer drops to about 1/3, indicating that the formation of these extremely low vapour pressure compounds is efficiently suppressed in the presence of isoprene. **b:** Both the total HOM (monomers+dimers, circles) and HOM dimers (squares, molecular mass > 370 Da) decrease with decreasing α-pinene turnover. Here [OH] was varied in two different ways: i) by decreasing the OH production rate, i.e. by decreasing the photolysis of ozone ($J(O^1D)$, blue) and ii) by adding increasing amounts of isoprene (red). In the presence of isoprene HOM decrease more strongly, mainly because the product scavenging is suppressing the α-pinene HOM dimers. The total HOM from the two different experiments were normalized to 1 for better comparison. **c:** Estimate of the product scavenging effect on α-pinene HOM dimers by isoprene at turnover 5.0×10^7 cm^{-3} s^{-1} based on molecular mass weighted signals in the mass spectra (details in Figure S8). Data for α-pinene-only were interpolated from the nearest $J(O^1D)$ data (arrows in **b**). The reduction in total HOM mass is 33%, to which dimers (dark green) contribute 26% and monomers 7% (light green). Error bars show the s.d. of the averages over 31 data points. The suppression of α-pinene HOM dimers of 26% explains most of the 35% product scavenging derived from reduced SOA formation in Figure 1. The balance is a result of the reduced yield of HOM monomers and/or shifts in their volatility spectrum.

Figure 4: Suppression of α-pinene SOA in presence of CO illustrating the generality of the product scavenging effect.
a: comparison of three mass spectra taken in experiments with (orange [CO]=10 ppm, red [CO]=57 ppm) and without CO (blue). In the presence of [CO] > 10 ppm the dimer/monomer drops by more than 1/2, indicating that the formation of the dimers is efficiently suppressed in the presence of CO. Because of the high [CO] overall HOM are suppressed by factor of 4 and 5 respectively. **b:** The product scavenging effect reduces the α-pinene yield in the reaction system α-pinene & CO & OH in the presence of ammonium sulfate seeds. The actual SOA yield, calculated as actual organic mass/actual α-pinene consumption, decreases by more than 50%, when 40 ppm CO was added to the reaction system. CO concentrations were calculated from known inlet concentration, the flow rate through the RC and the reaction rate of CO with OH. Light colored data points show steady state averages, whereby horizontal error bars show the averaging interval; s.d. of the averages are of the same size or smaller than the symbols. Note, panels **a** and **b** were not taken from the same experiment: experiments to show HOM in the gas-phase and to show SOA suppression cannot be performed in optimal fashion under the same conditions. To measure the unperturbed HOM-MS, particle formation must be avoided. In contrast, mass formation and its suppression must be determined in presence of seed surface as HOM losses at the walls of the chamber have to be minimized. Therefore, the experiment to measure the HOM-MS was performed without seed aerosol whereas ammonium sulfate particles were added to measure the suppression of mass formation by CO. Otherwise the conditions of the experiments were similar.

Figure 5: Atmospheric implications of product scavenging and OH scavenging. Global model calculations showing that OH scavenging (OHS) and product scavenging (PS) in presence of isoprene reduce the photochemically derived MT-OH-SOA mass (red) significantly compared to the reference cases NoIso. For the calculation a 4% iSOA yield for acidic aerosols was applied (sum of the brownish bars). OHS is inherently considered in models as long as biogenic SOA (BSOA) formation is directly linked to the oxidant fields, but the new PS effect reduces the MT-OH-SOA even further. To illustrate the maximum potential PS effect it was also applied to ozone derived MT-O_3-SOA (orange, PSOx). In this case the iSOA gain for 1% iSOA yield on neutral aerosols (dark brown) would not be able to compensate for the loss of MT-SOA. We show the global average and results for regions with high and low isoprene emissions and high and low population density. The map shows isoprene emissions, green shaded in [mg m^{-2}] and the areas of the selected regions. All contributions are normalised to MT-OH-SOA of the respective NoIso case, when biogenic isoprene emissions were omitted in the model (suppl. section 8).

α-Pinene

α-Pinene + Isoprene

α-Pinene + Isoprene
OH re-adjusted

OH•

a

Δ α-pinene
Δ isoprene [ppb]

Isoprene adjustments

OH conc. [cm^{-3}]

Organics / SO_4^{2-}

Product scavenging

OH scavenging

B

C

D

-2 0 2 4 6 8 10 12

Duration since isoprene addition [h]

b

Neutral seed particles

Acidic seed particles

SOA yields

B
α-Pinene reference

C
Product & OH scavenging

D
Product scavening

B
α-Pinene reference

C
Product & OH scavenging

D
Product scavening

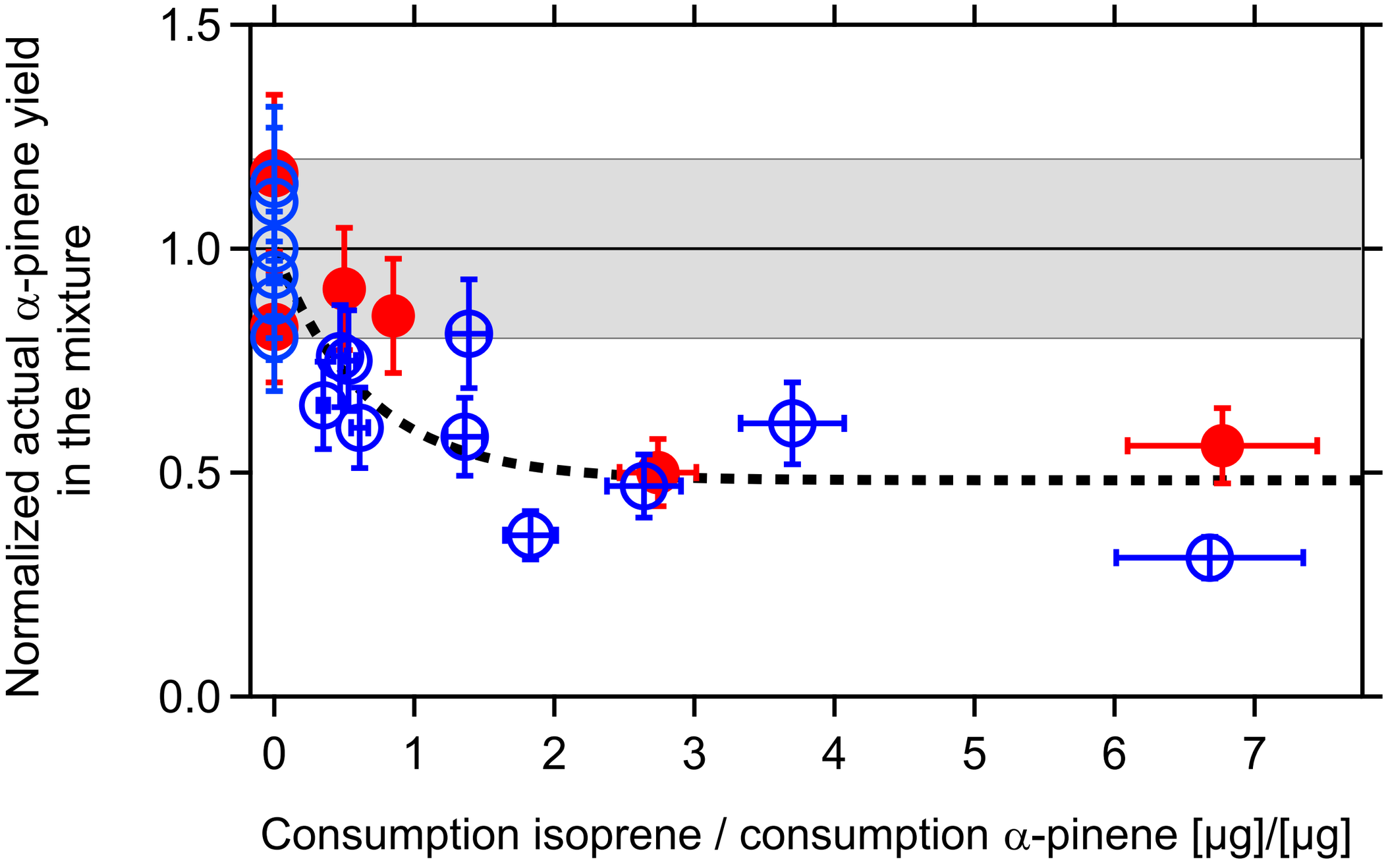
Normalized actual α-pinene yield
in the mixture
1.5
1.0
0.5
0.0
0
1
2
3
4
5
6
7
Consumption isoprene / consumption α-pinene [µg]/[µg]

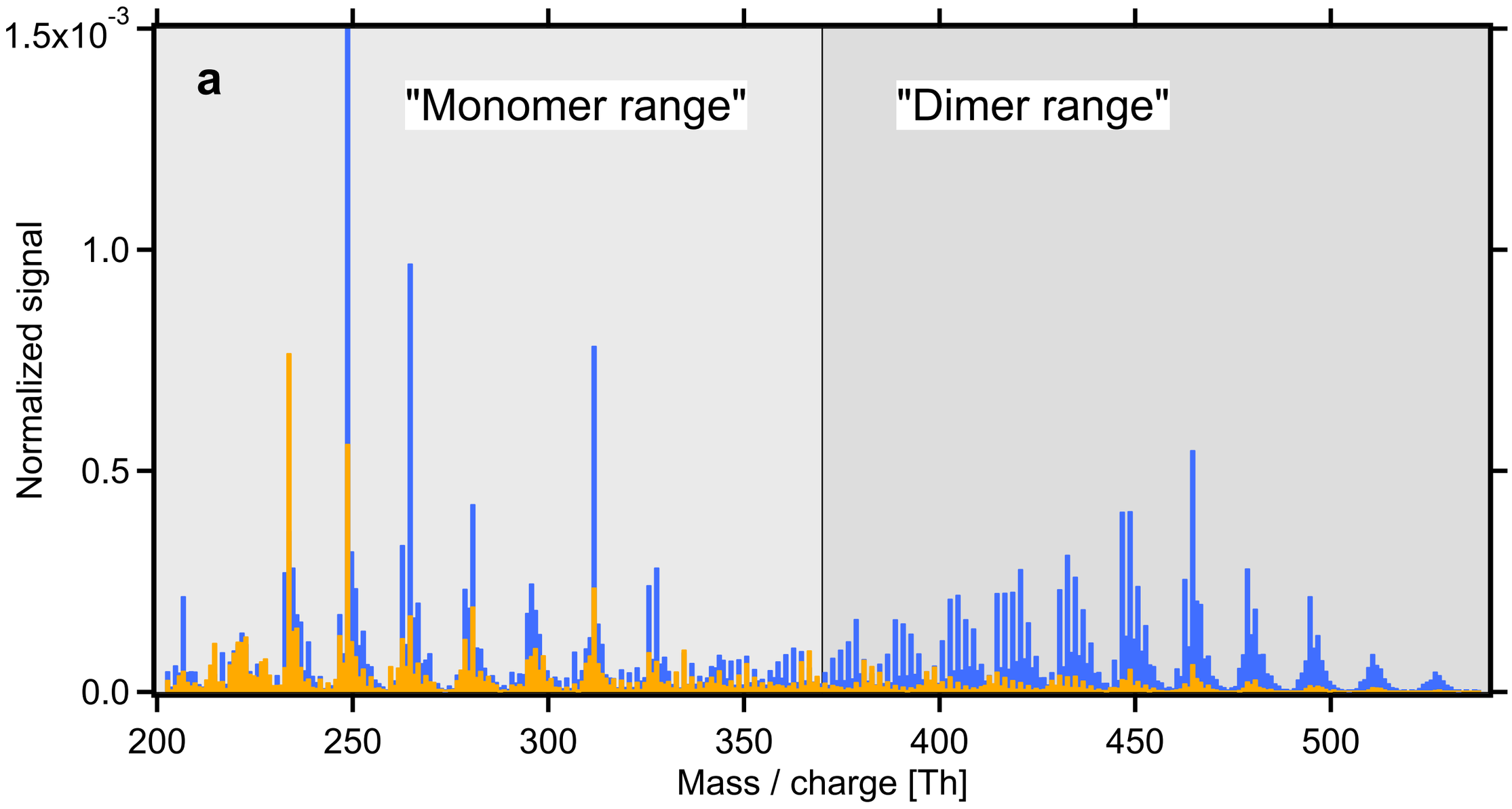

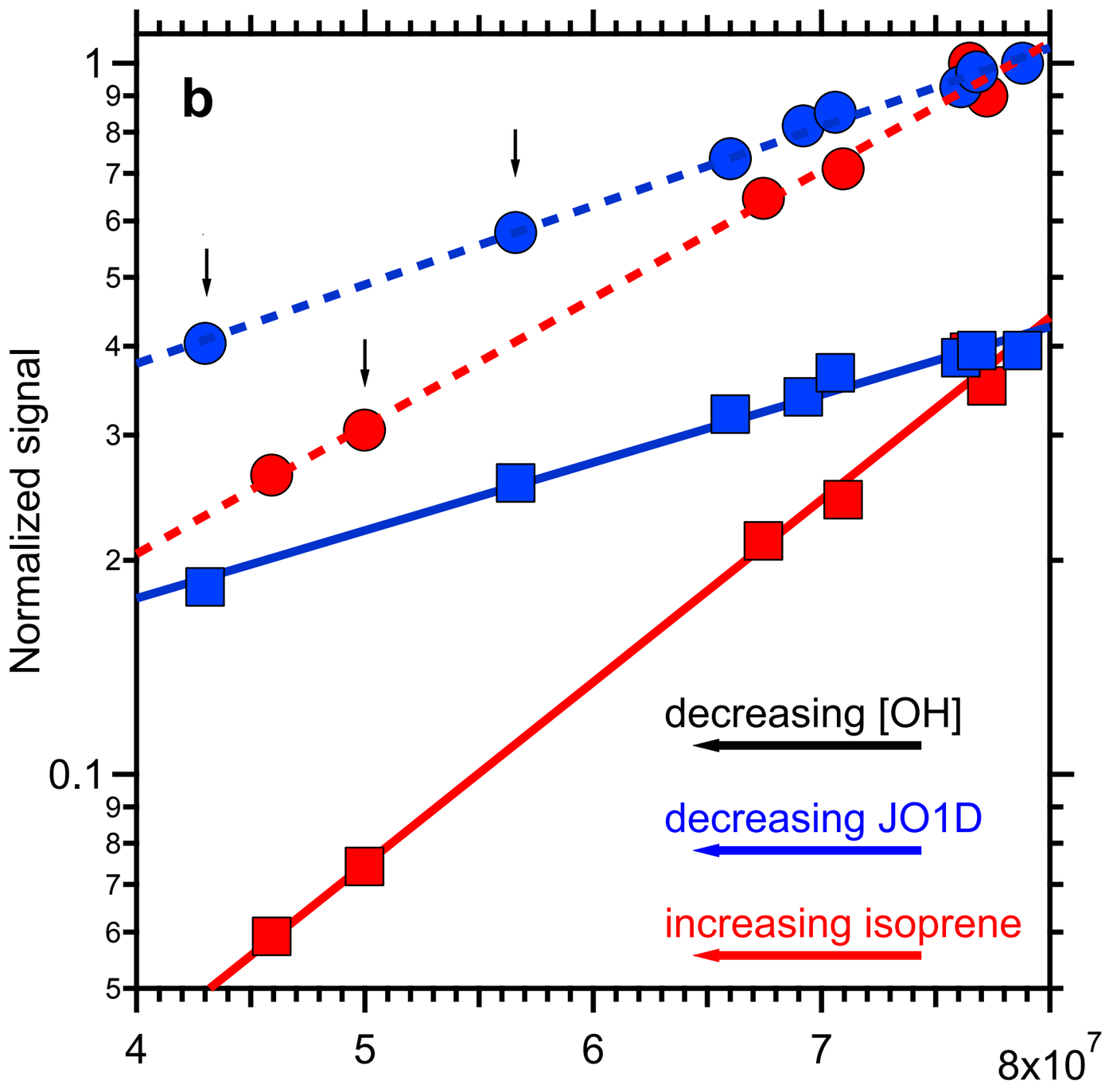

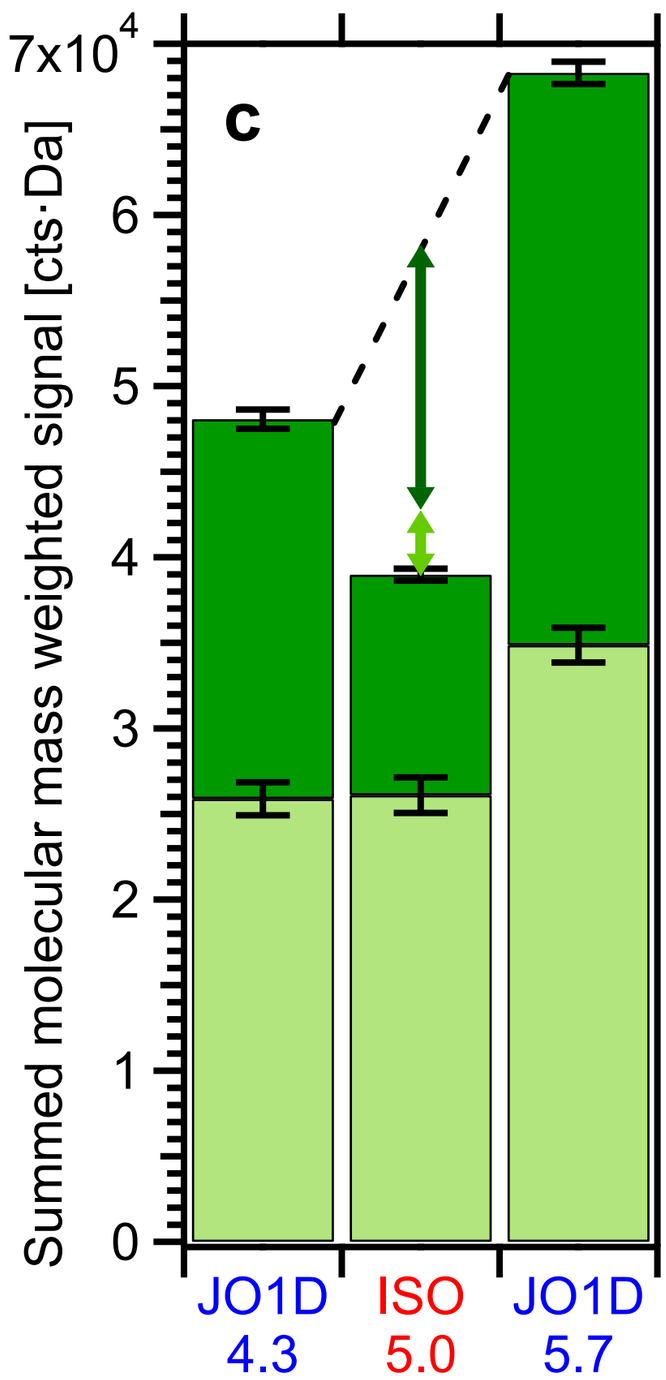

α-Pinene turnover: k_{OH}·[OH]·[α-pinene] [cm^{-3} s^{-1}] [·10^7 cm^{-3} s^{-1}]

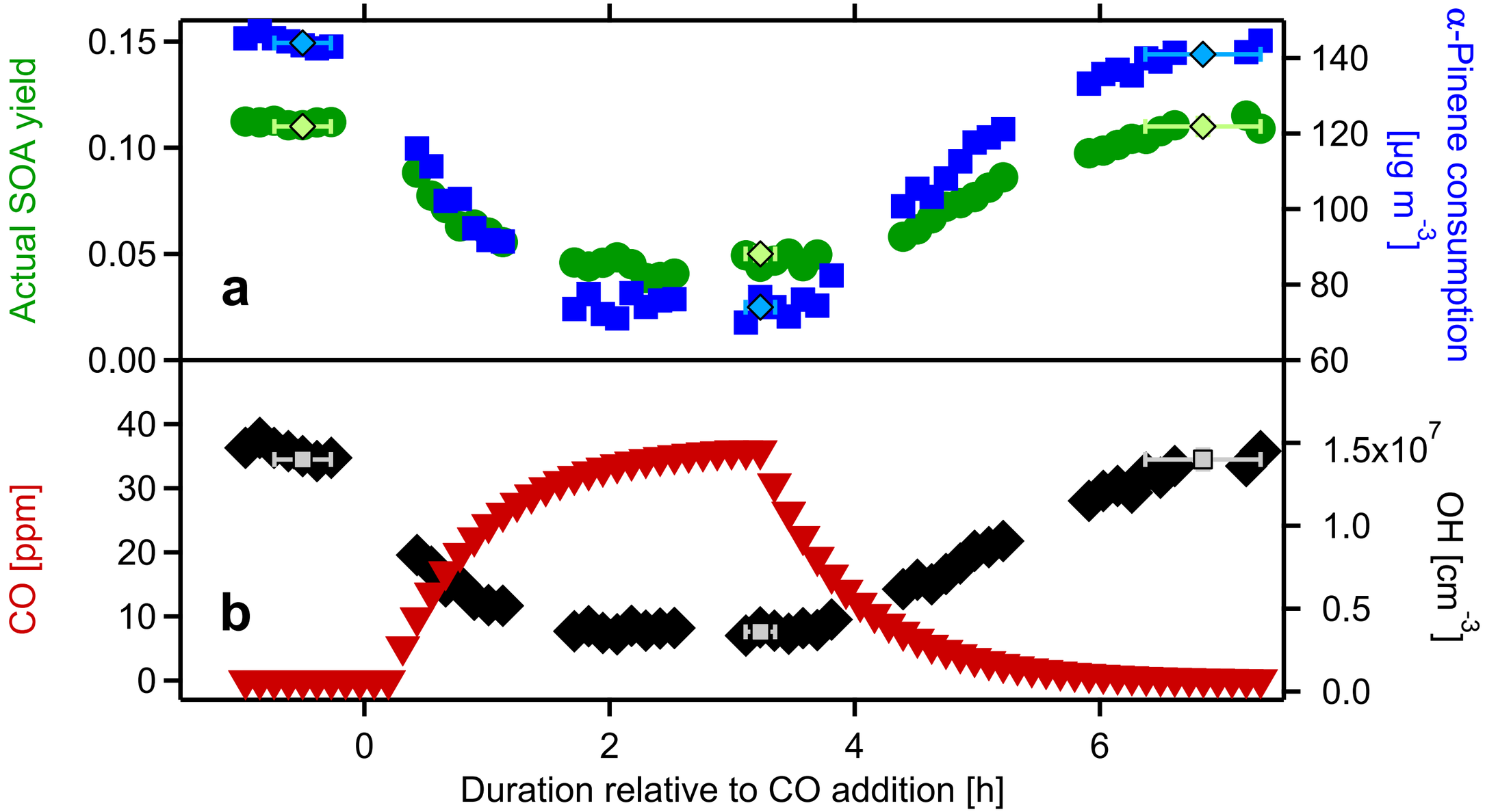
Actual SOA yield
0.15
0.10
0.05
0.00
a
α-Pinene consumption [μg m-3]
140
120
100
80
60
CO [ppm]
40
30
20
10
0
b
OH [cm-3]
1.5x10^7
1.0
0.5
0.0
0
2
4
6
Duration relative to CO addition [h]

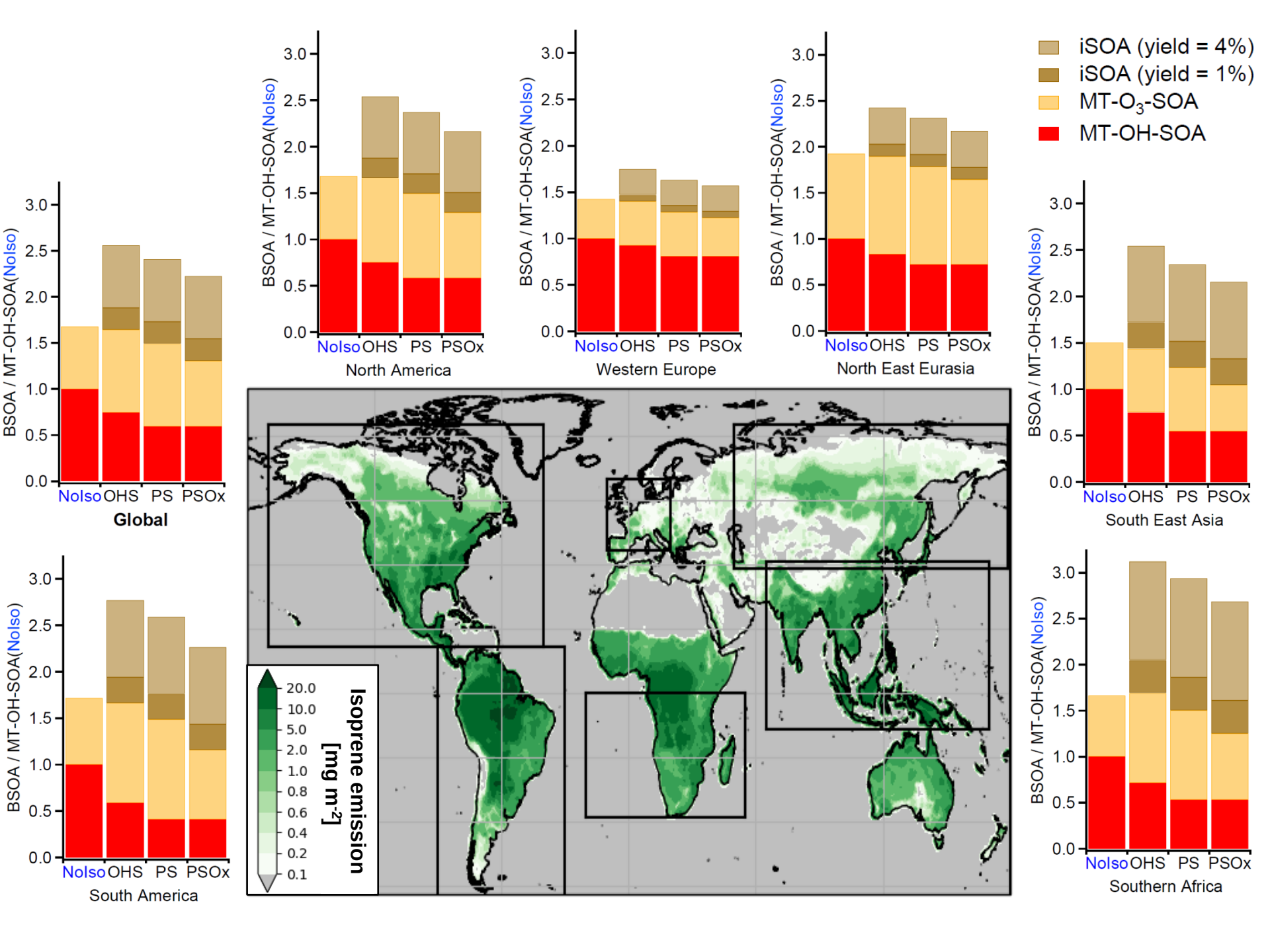
iSOA (yield = 4%)
iSOA (yield = 1%)
MT-O3-SOA
MT-OH-SOA
BSOA / MT-OH-SOA(NoIso)
NoIso OHS PS PSOx
Global
North America
Western Europe
North East Eurasia
South East Asia
South America
Southern Africa
Isoprene emission [mg m-2]
20.0
10.0
5.0
2.0
1.0
0.8
0.6
0.4
0.2
0.1

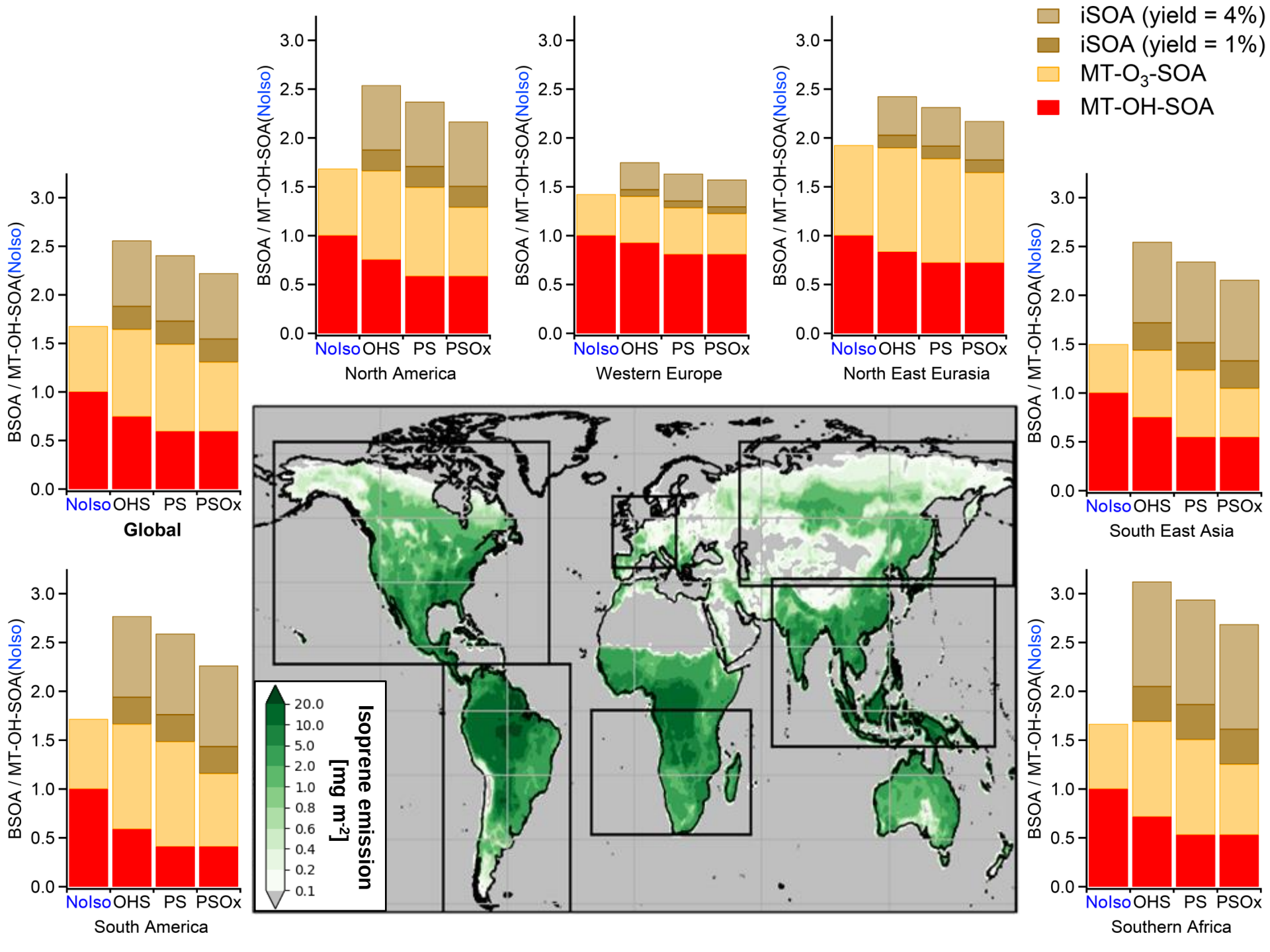
iSOA (yield = 4%)
iSOA (yield = 1%)
MT-O3-SOA
MT-OH-SOA
BSOA / MT-OH-SOA(NoIso)
NoIso OHS PS PSOx
Global
North America
Western Europe
North East Eurasia
South East Asia
South America
Southern Africa
Isoprene emission [mg m-2]
20.0
10.0
5.0
2.0
1.0
0.8
0.6
0.4
0.2
0.1

Supplement to

Secondary organic aerosol reduced by mixtures of atmospheric vapours

1. Jülich Plant Atmosphere Chamber (JPAC)

The experiments were performed in a continuously stirred flow reactor with a volume of 1450 L, which is part of the Jülich Plant Atmosphere Chamber (JPAC). The reaction chamber (RC) is located in a thermally stabilised housing and was used in the latest extension stage as described previously[22,45,46] and sketched in Figure S1. In short: supply air was pumped through the RC at a total flow of 30-35 L min^{-1} resulting in a residence time of 40-50 min. The supply flow was split into half onto two separate lines for the reactants in order to prevent reactions in the supply lines. Ozone and water vapour were added to one of the air streams entering the RC, while the other inlet stream contained the VOC. Here we studied α-pinene (Aldrich, purity > 99%) and isoprene (Aldrich, purity > 99%) and mixtures of both. VOC, α-pinene and isoprene, were introduced into the RC by flowing clean nitrogen over diffusion sources[47]. Since we prepare the clean air by purifying outside air including catalytic combustion, there is always a residual NO_X concentration of about 300 ppt in the RC. Here, all experiments were performed under low NO (NO < 30ppt) and low NO_2 (NO_2 < 300ppt) conditions. Steady state concentrations of the VOC during the experiments are given in Table S1. In few accompanying experiments we used β-pinene (Aldrich, purity > 99%), CO (Prüfgas, 4000 ppm in N_2, Linde AG) and CH_4 (purity, 99.9995 %, Linde AG).

OH radicals were produced by O_3 photolysis at 254 nm in the presence of water vapour. The forming excited O^1D atoms react with water vapour in the chamber and generate OH radicals in a concentration range of $1\text{-}10 \cdot 10^7$ cm^{-3}. The OH concentration [OH] is regulated by the source strength i.e. by shielding the UV light shining into the chamber by two movable glass shields which are opaque to light at 254 nm allowing for different length of the open gap of the UV. The actual OH steady state concentration $[OH]_{ss}$ depended also on the VOC source strength, i.e. even if O_3 flow into the chamber and TUV gap were held constant, O_3 steady state concentration and OH concentration varied depending on the reactivity provided by α-pinene, isoprene, and their mixtures. The $[OH]_{ss}$ are listed in Table S1.

Several instruments were used to measure the chamber experiment conditions. Ozone was measured by two UV photometric devices: Thermo Environment 49 or Ansyco, O3 42M ozone analyser. To monitor humidity dew point mirrors were used at both inlet and outlet flows. All instruments could be switched from outlet to inlet to follow the differences caused by reactions in the chamber.

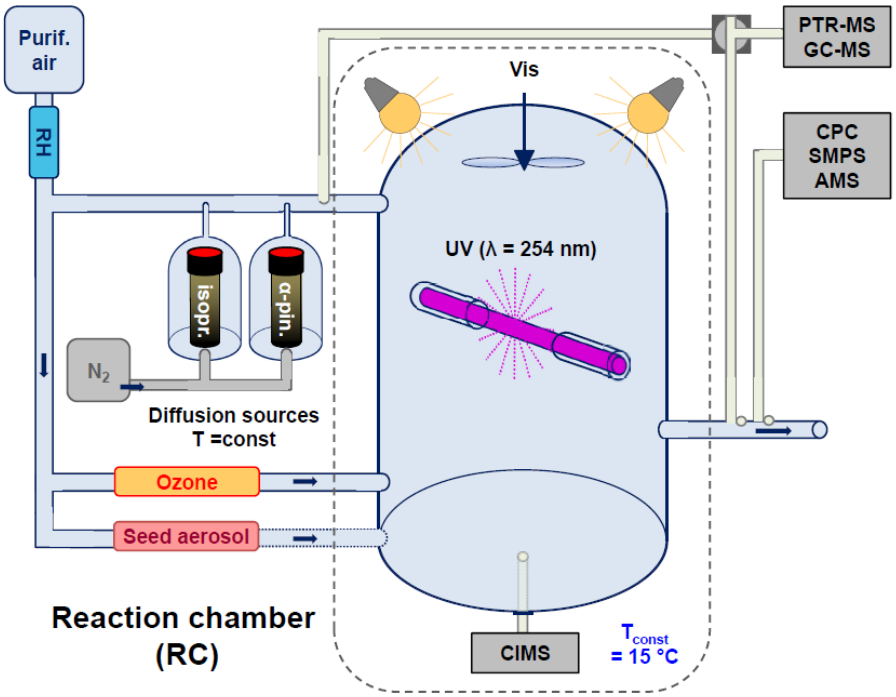

Figure S1: Schematic of the JPAC Reaction Chamber (RC).
α-pinene and isoprene were introduced to the RC by flowing clean nitrogen over diffusion sources. Ozone and water, in separate flows, provided O_3 concentrations around 60 ppb and relative humidity of about 60% at 15°C. The total flow amounted to 30 L/min, resulting in a residence time of about 50 min. in the RC of 1450L volume. Concentrations of α-pinene and isoprene, as well as oxidations products, were measured at inlet and outlet of the RC by GC-MS and PTR-MS. By switching on the UV lamp, O_3 was photolysed and O^1D atoms reacted with water vapour to give OH at concentrations in a range of $1\text{-}10 \cdot 10^7$ cm^{-3}. The OH source strength was regulated by the two movable glass shields allowing for different length of the gap for the UV. HOM were detected by a NO_3^--TOF-CIMS directly under the RC. Particle number concentration and number size distribution were determined by a Condensation Particle Counter (CPC) and by a Scanning Mobility Particle Sizer (SMPS). The particle composition was measured by an aerosol mass spectrometer (HR-TOF-AMS).

The number concentration of particles and their number size distribution were measured at the outlet of the RC by a CPC (TSI 3783) and by an SMPS (TSI 3081 electrostatic classifier combined with TSI 3025 CPC). Particle composition was measured using a high-resolution time of flight aerosol mass spectrometer (HR-ToF-AMS). A modified version of the HR-ToF-AMS (Aerodyne Inc., hereafter referred to as AMS) was used[48]. Briefly an AMS allows the mass spectrometric online investigation of aerosol particle composition after substantial reduction of the gas phase. The AMS was calibrated for ionization efficiency with NH_4NO_3 and $(NH_4)_2SO_4$ aerosol and particle size calibrated using polystyrene latex standards (PSL, Duke Scientific Corporation, Palo Alto CA) of different sizes between 81 nm and 596 nm. Compound specific relative ionization efficiencies (RIE; ionization efficiency relative to NO_3^-) were used. For NH_4^+ and SO_4^{2-}, RIE was determined from the respective calibration close to each experiment and was

found to be in the range of 3.75 – 4.2 and 0.83 – 1.03, respectively. RIE for particulate water was set to 2.0[49]. The RIE for organics was kept at the standard value of 1.4[50]. For the determination of the collection efficiency (CE) the volume concentration was calculated from SMPS measurements and multiplied by a density to yield the mass concentration. The density was calculated from the relative ratios of ammonium sulfate (density=1.77g cm^{-3}), particulate water (density=1 g cm^{-3}) and organics (density=1.4 g cm^{-3}). The ratio of total measured mass from AMS (sum of organics, sulfate, ammonium and particulate water) to mass derived from SMPS gave then the respective CE. The CE was between 0.2 and 0.3 since the ammonium sulfate mass fraction of the aerosol phase was typically > 60%. An average CE was determined and applied for each experiment. The data analysis focused on the mass concentration of the organic fraction and the organic/SO_4 ratio.

Highly oxygenated multifunctional molecules (HOM) are formed in the gas-phase in the RC by OH reaction and ozonolysis of α-pinene. HOM were measured by an Atmospheric Pressure interface High Resolution Time of Flight Mass Spectrometer (APi-TOF-MS, Aerodyne Research Inc. & Tofwerk AG)[51]. The anion NO_3^- is able to form a cluster with the expected HOM.[52] Therefore the APi-TOF-MS was equipped with a NO_3^--Chemical Ionization (CI) source[53,54] (A70 CI-inlet, Airmodus Ltd). The NO_3^--TOF-CIMS was directly placed under the RC within the thermo-stabilised housing of the chamber, i.e., it was operated at stable temperature conditions. Reagent ions $^{14}NO_3^-$ were formed from HNO_3 (Merck) ionized by an in-line ^{241}Am foil. The vial with the nitric acid and all lines were also placed within the thermo-stabilised housing.

The length of sampling line (ID 8 mm) was about 30 cm and the sample flow from the RC into the CI source was 10 L/min. The flow into the NO_3^-- TOF-CIMS was thereafter reduced to 0.8 L/min by passing a critical orifice. Differential pumping by a scroll pump and a three-stage turbo pump decreased sequentially the pressure from 1015 mbar in the CI region to 10^{-6} mbar in the Time of Flight region. After passing the critical orifice the ions are guided by segmented quadrupole mass filters and electrical lenses in the TOF extraction region. Collisions between ions and gas molecules will take place, but the energies are tuned low enough that only weakly bound clusters (e.g. water clusters) will fragment. After extraction into the TOF region the ions are separated by their different flight times depending on their mass-to-charge (*m/z*) ratio.

There is strong indication that the sensitivity of the NO_3^--TOF-CIMS is fairly similar for all HOM species once a certain degree of functionalization is achieved (two –OH or –OOH groups in addition to two carbonyl groups)[22,55]

Studies with cyclopentane showed that HOM with 5 C atoms and 6 O atoms or more can be detected. However, we are able to detect HOM with less than 6 O-atoms in molecules with 7 or more C-atoms[45]. Thus, the polarisability of a molecule may play a role in addition to directional interactions of functional groups with the NO_3^- ion.

Table S1: Overview of a-pinene and a-pinene + isoprene experiments

$\frac{\Delta\text{Isoprene [µg]}}{\Delta\text{α-Pinene [µg]}}$	[OH] [cm^{-3}]	Mixing ratio α-pinene in RC [ppb]	α-pinene consumption [µg m^{-3}]	Isoprene consumption [µg m^{-3}]	Organic mass [µg m^{-3}]	Particle Surface S_{tot} [m^2 m^{-3}]	Wall loss corr. factor $1/F_{pHOM}$	Corr. organic mass [µg m^{-3}]	Yield iso.+α-pin.	Yield α-pin.
α-pinene only										
neutral seeds										
-	$7.1\cdot10^7 \pm 6.9\cdot10^6$	1.2	68 ± 0.7	0	5.8	$2.660\cdot10^{-4}$	1.768	10.3	-	0.152
-	$3.2\cdot10^7 \pm 1.6\cdot10^6$	2.1	56 ± 1.2	0	6.3	$4.157\cdot10^{-4}$	1.529	9.6	-	0.172
-	$3.6\cdot10^7 \pm 2.3\cdot10^6$	1.9	55 ± 1.9	0	6.6	$3.166\cdot10^{-4}$	1.646	10.9	-	0.197
-	$7.1\cdot10^7 \pm 7.8\cdot10^6$	1.1	64 ± 2.3	0	8.3	$8.472\cdot10^{-4}$	1.241	10.3	-	0.162
-	$4.9\cdot10^7 \pm 5.1\cdot10^6$	1.5	65 ± 2.0	0	7.2	$8.451\cdot10^{-4}$	1.251	9.0	-	0.138
-	$4.8\cdot10^7 \pm 4.6\cdot10^6$	1.5	61 ± 3.0	0	6.5	$8.451\cdot10^{-4}$	1.241	8.1	-	0.133
-	$4.0\cdot10^7 \pm 3.0\cdot10^6$	1.8	60 ± 2.7	0	13.3	$1.878\cdot10^{-3}$	1.113	14.8	-	0.246
-	$2.4\cdot10^7 \pm 3.5\cdot10^6$	2.8	53 ± 3.1	0	8.8	$1.340\cdot10^{-3}$	1.152	10.1	-	0.190
-	$2.7\cdot10^7 \pm 5.4\cdot10^6$	2.5	55 ± 2.3	0	9.6	$1.482\cdot10^{-3}$	1.138	10.9	-	0.197
acidic seeds										
-	$1.0\cdot10^8 \pm 1.9\cdot10^7$	0.8	68 ± 2.5	0	8.1	$1.102\cdot10^{-3}$	1.186	9.7	-	0.142
-	$4.4\cdot10^7 \pm 6.3\cdot10^6$	1.7	61 ± 1.0	0	10.7	$1.344\cdot10^{-3}$	1.152	12.3	-	0.201
α-pinene & isoprene										
neutral seeds										
0.35	$2.8\cdot10^7 \pm 2.0\cdot10^6$	2.4	55 ± 2.7	19 ± 0.2	3.7	$6.399\cdot10^{-4}$	1.318	4.9	0.066	0.090
0.61	$7.9\cdot10^6 \pm 6.1\cdot10^5$	5.7	37 ± 1.3	23 ± 0.8	3.6	$1.287\cdot10^{-3}$	1.158	4.2	0.070	0.113
0.47	$2.3\cdot10^7 \pm 4.3\cdot10^6$	3.0	57 ± 2.0	27 ± 3.3	2.8	$1.431\cdot10^{-4}$	2.404	6.6	0.079	0.116
0.51	$2.3\cdot10^7 \pm 1.9\cdot10^6$	2.8	53 ± 0.9	27 ± 0.4	6.4	$1.406\cdot10^{-3}$	1.144	7.3	0.090	0.136
0.53	$3.4\cdot10^7 \pm 1.7\cdot10^6$	2.2	62 ± 0.5	33 ± 0.3	3.3	$1.810\cdot10^{-4}$	2.131	7.1	0.075	0.115
1.36	$1.1\cdot10^7 \pm 7.4\cdot10^5$	4.8	41 ± 2.3	56 ± 0.5	5.1	$1.390\cdot10^{-3}$	1.147	5.9	0.061	0.143
1.39	$1.3\cdot10^7 \pm 8.7\cdot10^5$	4.2	43 ± 1.9	60 ± 0.7	4.4	$3.802\cdot10^{-4}$	1.550	6.9	0.067	0.160
1.83	$9.0\cdot10^6 \pm 7.1\cdot10^5$	5.3	38 ± 3.0	70 ± 1.5	1.7	$6.575\cdot10^{-4}$	1.311	2.2	0.021	0.058
2.64	$1.1\cdot10^7 \pm 1.1\cdot10^6$	4.8	40 ± 3.0	105 ± 0.6	1.9	$7.496\cdot10^{-4}$	1.271	2.5	0.017	0.062
3.70	$7.0\cdot10^6 \pm 4.3\cdot10^5$	6.0	30 ± 1.7	110 ± 1.4	1.8	$3.114\cdot10^{-4}$	1.680	3.0	0.022	0.102
6.68	$2.7\cdot10^6 \pm 3.2\cdot10^5$	8.8	20 ± 3.3	137 ± 13.3	0.8	$6.413\cdot10^{-4}$	1.318	1.0	0.007	0.050
acidic seeds										
0.48	$4.3\cdot10^7 \pm 4.0\cdot10^6$	1.7	61 ± 1.1	29 ± 0.2	15.2	$1.489\cdot10^{-3}$	1.137	17.2	0.191	0.282
0.50	$1.3\cdot10^7 \pm 1.2\cdot10^6$	4.4	46 ± 2.9	23 ± 0.4	7.3	$1.315\cdot10^{-3}$	1.155	8.4	0.122	0.183
0.85	n.a.	4.7	46 ± 1.0	39 ± 0.4	4.5	$1.034\cdot10^{-3}$	1.205	5.5	0.065	0.120
2.74	$3.6\cdot10^7 \pm 2.3\cdot10^6$	11.3	57 ± 3.2	155 ± 2.2	5.9	$6.915\cdot10^{-4}$	1.369	8.1	0.038	0.143
6.77	$7.1\cdot10^7 \pm 7.8\cdot10^6$	14.2	40 ± 2.7	272 ± 8.4	4.7	$6.600\cdot10^{-4}$	1.386	6.5	0.021	0.161

To control whether or not peaks in the NO_3^--TOF-CIMS mass spectra originated from oxidation of the added VOC, blank experiments without VOC addition were performed. Ozone was left in the chamber in case of peaks originating from ozonolysis of impurities. Some of the peaks in the mass spectra were abundant also in absence of VOC and likely arise from fluorinated contaminants. All peaks observable without VOC addition were excluded from interpretation.

VOC and their oxidation products were measured by a high sensitivity Proton-Transfer-Reaction Mass-Spectrometer (PTR-MS, IONICON). The technique is described in the literature[56]. Calibrations for α-pinene and isoprene were performed by using diffusion sources[57]. The PTR-MS was operated at 2 min time resolution and switched every 25 min between the inlet and the outlet of JPAC. The sampling lines consisted of ~10 m long PFA tubing of 4 mm inner diameter and were heated to 60°C. The sampling flow rate was 500 mL/min. The difference between inlet and outlet signal for α-pinene at *m/z* 137 was used to determine the OH concentration.

Most of the experiments were performed in the presence of seed particles to provide surfaces for condensing the oxidation products of α-pinene and isoprene in order to overcome the nucleation

barrier for secondary organic aerosol formation. The seed aerosols were generated by a TSI 3076 constant output aerosol generator with subsequent drying to RH<30% by diffusion dryers filled with silica gel. As neutral seeds we used ammonium sulfate particles, which were generated by spraying an aqueous ammonium sulfate solution. Acidic seeds were generated by spraying ammonium bisulfate solutions which were doped with some H_2SO_4 to guaranty acidity. The latter was assured by monitoring the molar NH_4/SO_4 ratio being <1 by AMS. In the evaluation of the seeded experiments the organic fraction of the aerosols observed by AMS was normalized to sulfate in order to correct for fluctuations of the particle concentration thus the condensation sink in the RC. Fluctuations arose from the long term instabilities in the particle generation process. Experiments for studies of the gas-phase composition were performed in absence of seed aerosols.

Because of the vigorous ongoing debate in the literature about the yield of isoprene and its role for SOA formation (e.g.[58] and references therein), we performed also experiments with isoprene only. An overview of the experiments with neutral and acidic seeds is given in Table S2. We refer to isoprene yields determined in our setup in the following discussions.

Table S2: Isoprene SOA yields on neutral and acidic aerosols in JPAC

Experiment Qualifier	[OH] [cm^{-3}]	Mixing ratio isoprene in RC [ppb]	Isoprene consumption [$\mu g\ m^{-3}$]	Organic mass [$\mu g\ m^{-3}$]	Particle Surface S_{tot} [$m^2\ m^{-3}$]	Wall loss corr. factor $1/F_{pHOM}$	Background offset [$\mu g\ m^{-3}$]	Corr. organic mass [$\mu g\ m^{-3}$]	Yield corrected
isoprene neutral seeds									
1	$2.4\cdot10^7 \pm 6.7\cdot10^5$	10.3 ± 0.2	139.0 ± 0.7	2.48 ± 0.05	$1.50\cdot10^{-3}$	1	1.03	1.4	0.01
2	$1.2\cdot10^7 \pm 5.8\cdot10^5$	18.1 ± 0.7	172.2 ± 1.9	2.51 ± 0.08	$1.48\cdot10^{-3}$	1	1.06	1.5	0.01
3	$1.6\cdot10^6 \pm 9.7\cdot10^4$	55.3 ± 1.0	227.3 ± 2.9	2.31 ± 0.05	$1.45\cdot10^{-3}$	1	1.02	1.3	0.01
4	$1.5\cdot10^6 \pm 7.8\cdot10^4$	201.2 ± 7.7	242.2 ± 21.8	2.05 ± 0.09	$1.45\cdot10^{-3}$	1	1.13	0.9	0.00
isoprene acidic seeds									
5	$5.68\cdot10^7 \pm 1.1\cdot10^7$	1.5 ± 0.2	67.1 ± 0.6	4.31 ± 0.14	$1.35\cdot10^{-3}$	1.19	1.46	3.66	0.05
6	$2.35\cdot10^7 \pm 9.6\cdot10^6$	14.1 ± 0.3	98.1 ± 0.9	4.18 ± 0.07	$1.26\cdot10^{-3}$	1.20	1.35	3.67	0.04
7	$6.10\cdot10^6 \pm 2.7\cdot10^6$	38.1 ± 0.7	121.2 ± 1.9	4.14 ± 0.08	$1.29\cdot10^{-3}$	1.20	1.31	3.64	0.03
8	$2.28\cdot10^6 \pm 4.2\cdot10^4$	86.9 ± 0.6	153.3 ± 1.7	3.52 ± 0.08	$1.33\cdot10^{-3}$	1.19	1.27	2.92	0.02
9	$2.73\cdot10^6 \pm 8.9\cdot10^4$	73.6 ± 1.0	155.0 ± 2.9	3.48 ± 0.10	$1.41\cdot10^{-3}$	1.18	1.65	2.46	0.02
10	$1.24\cdot10^6 \pm 4.0\cdot10^4$	258.7 ± 2.4	252.2 ± 6.7	2.50 ± 0.06	$1.30\cdot10^{-3}$	1.20	1.22	1.77	0.01
11	$1.30\cdot10^6 \pm 4.6\cdot10^4$	261.0 ± 2.4	262.0 ± 6.9	2.54 ± 0.11	$1.30\cdot10^{-3}$	1.20	1.11	1.93	0.01

2. SOA yield, its definition in mixtures and a perspective on OH scavenging

Here we illustrate the main controlling parameters of photochemical SOA mass formation in precursor mixtures. For clarity we will simplify our approach by assuming constant SOA yields prior to consideration of variable yields in section 3. In this discussion, as in our study, we represent the mixed state in the atmosphere by mixtures of isoprene, the major biogenic VOC[7] with a SOA yield of the order of a few percent (according to our observations in JPAC, Table S1 and S2), and α-pinene, the most abundant monoterpene[7] with a SOA yield of 15% or more.

Considering α-pinene in isolation being oxidised by OH, the particulate organic mass Δ[SOA] generated in a time interval Δt by definition is given by consumption of α-pinene during Δt multiplied by the α-pinene SOA yield (y_{AP}). The consumption of α-pinene Δ[AP] is time dependent and depends on the concentration of α-pinene $[AP]_{ss}$ and the concentration of $[OH]_{ss}$, which are assumed to be in a steady state indicated by the subscript ss (Eq. 1). This is the situation for many instances in the atmosphere, where sources and chemical losses balance over a time period of hours, but also in our RC.

$$\Delta[SOA]_{AP} = y_{AP} \cdot \Delta[AP]$$
$$\Delta[AP] = k_{AP} \cdot [OH]_{ss} \cdot [AP]_{ss} \cdot \Delta t \quad (1)$$

In the presence of isoprene a second component $\Delta[SOA]_{Iso}$ contributes to SOA formation (Eq 2):

$$\Delta[SOA]_{Iso} = y_{Iso} \cdot \Delta[Iso]$$
$$\Delta[Iso] = k_{Iso} \cdot [OH]_{ss} \cdot [Iso]_{ss} \cdot \Delta t \quad (2)$$

The formation of total organic mass Δ[SOA] is generally assumed to be given by:

$$\Delta[SOA] = y_{AP} \cdot \Delta[AP] + y_{Iso} \cdot \Delta[Iso]$$
$$\Delta[SOA] = \left(y_{AP} \cdot k_{AP} \cdot [OH]_{ss} \cdot [AP]_{ss} + y_{Iso} \cdot k_{Iso} \cdot [OH]_{ss} \cdot [Iso]_{ss}\right) \cdot \Delta t \quad (3)$$

In Eq. 3, y_{AP} is unaffected by the presence of isoprene and vice versa y_{iso} is unaffected by the presence of α-pinene. The SOA yield for a mixture of α-pinene and isoprene, y_{mix}, can then be defined by Eq. 4 using the consumption of both VOC.

$$\frac{\Delta[SOA]}{\left(k_{AP} \cdot [OH]_{ss} \cdot [AP]_{ss} + k_{Iso} \cdot [OH]_{ss} \cdot [Iso]_{ss}\right) \cdot \Delta t} = y_{mix} \quad (4)$$

Using the definition for y_{mix} in Eq. 4, it is obvious that it depends on the composition of the mixture. Starting from α-pinene alone and then adding more and more isoprene leads to a steady decrease of y_{mix}. The formed SOA mass is related to the total VOC consumption and the higher the contribution of isoprene consumption to the total consumption, the lower is y_{mix}. In the atmosphere, $[OH]_{ss}$ depends on many parameters and may not solely depend on the presence of isoprene.[59,60] We will differentiate two cases, either the presence of isoprene lowers the $[OH]_{ss}$ because it adds to the net chemical sink of OH, or $[OH]_{ss}$ depends more strongly on other parameters and remains about constant.

If the presence of isoprene lowers $[OH]_{ss}$, $\Delta[SOA]$ and y_{mix} will decrease in the mixture and should be lower than that for α-pinene alone (for the same $[AP]_{ss}$). This effect follows by

application of linear mixing rules (Eq. 5), which describes the individual contribution of each component to the total consumption, weighted by its respective yield.

$$y_{mix} = y_{AP} \cdot \frac{k_{AP} \cdot [OH]_{ss} \cdot [AP]_{ss}}{k_{AP} \cdot [OH]_{ss} \cdot [AP]_{ss} + k_{Iso} \cdot [OH]_{ss} \cdot [Iso]_{ss}} + y_{Iso} \cdot \frac{k_{Iso} \cdot [OH]_{ss} \cdot [Iso]_{ss}}{k_{AP} \cdot [OH]_{ss} \cdot [AP]_{ss} + k_{Iso} \cdot [OH]_{ss} \cdot [Iso]_{ss}} \quad (5)$$

As stated above, we observed a yield of isoprene of roughly an order of magnitude smaller than that of α-pinene in the presence of neutral preexisting aerosol or about a factor of 3 smaller with acidic aerosol (Tables S1 and S2, Figure S2, blue or red shaded ranges). The OH suppression by isoprene could lead to a reduction of SOA mass formation over certain regions of the world. Furthermore, as a result of the partitioning according to Raoult's law[61-63] the yield will be even smaller if less SOA is formed, which slightly enhances the OH suppression effect. (As the model results in section 8 illustrate the amount of SOA formed in real mixtures is more complex and depends on the specific concentrations of the precursors and their coupling to the oxidant fields.)

In case of constant $[OH]_{ss}$, *a priori* the SOA mass produced from α-pinene should be the same, independent on the presence of isoprene. If isoprene is present, isoprene oxidation adds to SOA mass and the total mass of SOA would become larger despite the small yield of isoprene. If we consider the partitioning effect the yields will even increase somewhat. In case of *isoprene not affecting $[OH]_{ss}$ we indeed would expect an increase of SOA mass* by the presence of isoprene, as postulated in the literature (e.g.[64,65]).

It can readily be envisaged that apart from isoprene there are wide ranges of components of varying reactivity and SOA yields that can comprise atmospheric mixtures in different environments. This means that components contributing significantly to SOA mass will influence the OH concentrations to different degrees. This will lead to a variety of degrees to which oxidant scavenging can influence SOA mass in the atmosphere.

The oxidant effect described so far affects only y_{mix}, the yields of the individual VOC in the mixture were assumed to be constant. If we consider that the SOA yield y_{AP} itself may be OH dependent, e.g. by oxidative ageing of the vapours (e.g.[31,32], references therein and section 6), the suppressing effect of isoprene will be even stronger. Regardless of whether the SOA formation is suppressed due to reduced availability of OH for reactions with the VOC, or by lower yields at lower OH concentrations, we call this phenomenon *OH scavenging* effect.

The *OH scavenging effect* due to linear mixing rules (Eq. 5) is included in the global model calculations presented in section 8 and its importance for SOA mass is evident. However linear mixing rules are not the topic of our mechanistic investigations. The focus of our mechanistic studies is the effect of isoprene on $y_{AP,}$ i.e. we newly discovered changes of y_{mix} on top of those obvious from applying linear mixing rules. There were two effects causing the decrease of y_{AP}

when adding isoprene: the OH dependence of y_{AP} – due to an *OH scavenging effect* – and the new *product scavenging effect*. The existence of a product scavenging effect will be derived by analysis of *SOA yields in mixtures* in the next section.

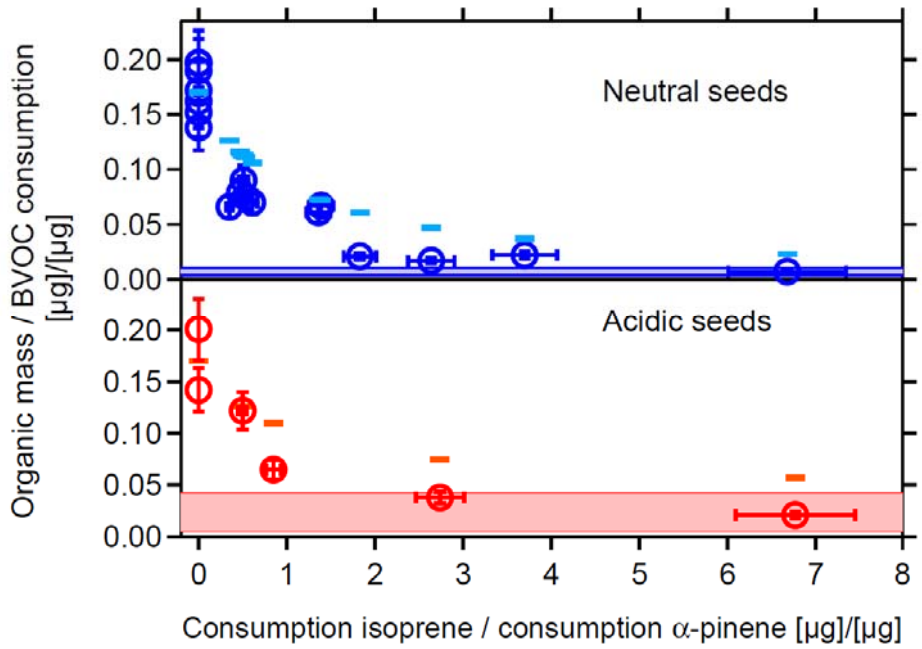

Figure S2: SOA yields of α-pinene & isoprene mixtures as a function of the relative consumption (isoprene / α-pinene) for neutral ammonium sulfate (blue circles) and acidic ammonium bisulfate seed aerosol (red circles).
The presence of isoprene lowers the steady state concentration of OH and in both cases reduces the SOA yield of the mixture. The light blue and the orange dashes show the expectation assuming linear mixing rules and constant yields (y_{AP}=0.17 for both and y_{Iso}=0.01 for neutral seeds and y_{Iso}=0.04 for acidic seeds). Blue shaded area: range of isoprene SOA yields in presence of neutral seed aerosols for pure isoprene reaction systems. Red shaded area: range of isoprene SOA yields in presence of acidic aerosols for pure isoprene reaction systems. Isoprene yields are higher on acidic seed aerosols. The scattering of the data for the pure reaction systems of α-pinene (circles at x = 0) and isoprene (shaded areas) is a result of experimental uncertainties as indicated by the error bars and also by variabilities in experimental reaction conditions (O_3, VOC, OH production).

3. New observations: SOA yield for isoprene α-pinene mixtures

Figure S2 shows that, with increasing ratios of isoprene/α-pinene consumption, i.e. larger excess of isoprene, SOA mass yield reduces by about on order of magnitude down to the yield of isoprene alone. Suppression of SOA mass and SOA mass yields by isoprene occurred in the presence of neutral as well as acidic seed aerosols (Figure S2). Herein we considered the summed consumption of both VOC to calculate y_{mix} (Eq. 4). The observed suppression effect was not fully compensated by accretion reactions of isoprene oxidation products in the particulate phase on

acidic seed particles.[12,35-37] In our case this led indeed to higher yields in presence of acidic aerosols and compensated for some of the suppression effects (Figure 1, and red data in Figure S2).

Simultaneous oxidation of VOC mixtures is the normal process in the atmosphere. It is not obvious how to reference the SOA mass formation to the consumption of VOC in the mixture when calculating the yield. In Figure S2 we presented the yield y_{mix} for the α-pinene/isoprene mixtures using the total BVOC consumption which, in our case, is the sum of the isoprene and the α-pinene consumption. The light blue markers in Figure S2 shows that we *a priori* should expect a drop of the SOA yield by reduction of $[OH]_{ss}$ (OH scavenging) for α-pinene/isoprene mixtures, assuming linear mixing rules. The ideal mixing line calculated by applying Eq. 5 is higher than the observations indicating, that *more than simple OH scavenging* occurs and y_{AP} seems to be affected by the presence of isoprene. The same is true for the acidic seed aerosols (red markers).

In the mixtures of "low yield" SOA forming isoprene and "high yield" SOA forming α-pinene studied here, it is also justified to reference the SOA yield to α-pinene alone as long as $y_{Iso} << y_{AP}$. Since this neglects the minor contribution of the isoprene SOA, it gives an upper limit for the SOA generated from α-pinene at the given conditions. Referencing solely to the actual consumption of α-pinene clarifies the role of α-pinene in the mixture since it reflects that not only $[OH]_{ss}$, and thus the actual α-pinene consumption was lowered by the presence of isoprene but also the SOA yield y_{AP} itself, as described in the main manuscript (Figure 2). The result is striking. Although isoprene must have contributed somewhat to the SOA mass, at least in the acidic case, the normalized yield is always smaller than unity, which means that the production of SOA from α-pinene is *less effective* in the presence of isoprene. We will show in our experiments that this effect is related to the behaviour of the recently discovered HOM and HOM dimers[22,51] and their removal from the pool of species contributing to SOA mass; we call this phenomenon *"product scavenging"*. The discovery of the product scavenging effect, leading to a negative effect on y_{AP} when adding e.g. isoprene is the core of this paper and it will challenge the concept of additive or enhanced SOA yield at constant [OH]. In the next section 4 we will describe the concepts to separate product scavenging and OH scavenging.

4. Experimental separation of OH scavenging and product scavenging

We have experimentally separated, isolated, and quantified the *OH scavenging* and the *product scavenging* effects. The key to this separation was the adjustment of the OH production and thus α-pinene consumption was adjusted during the particular measurements to obtain the *same* OH concentration $[OH]_{ss}$ in presence and absence of isoprene. Such OH adjustments are a unique feature of JPAC. We performed the experiments with neutral seeds (Figure 1A) and acidic seeds (Figure S3), in order to take into account that isoprene oxidation products can undergo condensed-phase accretion reactions in acidic environments (Figure S4).[35-37,66,67] As neutral seeds we used ammonium sulfate particles and as acidic seeds ammonium bisulfate doped with some extra H_2SO_4.

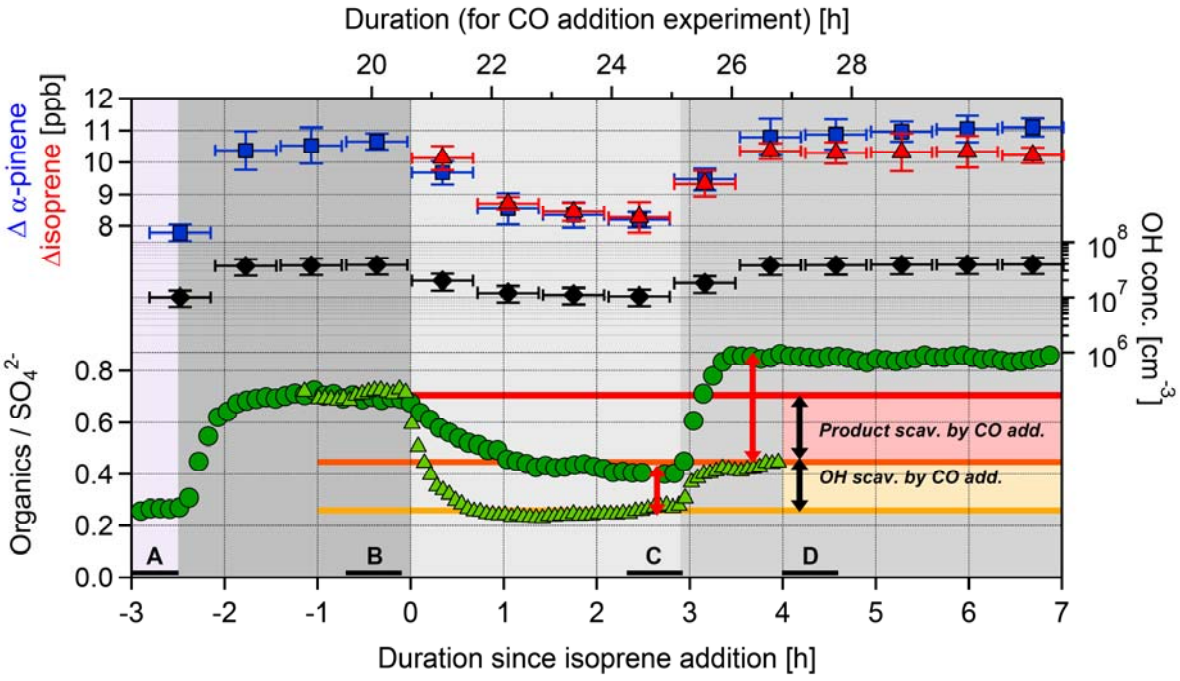

Figure S3: *Product scavenging* and *OH scavenging* effect in the presence of acidic ammonium bisulfate seed aerosols, by isoprene (dark green circles, lower time axis) and by CO (light green triangles, upper time axis). The dark grey area shows the reaction system α-pinene & OH as a reference. In the beginning of the light grey area isoprene was introduced into the chamber, in the beginning of the medium grey area OH was re-adjusted to the same value as in the dark grey period. The letters indicate periods of steady state for ozonolysis (A), α-pinene & OH (B), α-pinene & isoprene & OH (C); α-pinene & isoprene & [OH] adjusted (D). Values in Figure 1B are taken from these periods. The organic mass was normalized to sulfate mass in order to compensate for fluctuations of the seed aerosol generation and is shown as organic to sulfate ratio (organics/SO_4^{2-}, dark green circles and light green triangles).

Addition of isoprene (red triangles) lowered [OH] (black diamonds) and α-pinene consumption (Δ α-pinene, blue squares), leading to reduced formation SOA mass. Re-adjusting [OH] and α-pinene consumption induced enhanced SOA mass formation. This is different for the acidic seed aerosol compared to the neutral seed aerosol (Figure 1A). Later in the experiment (top axis) isoprene was removed and CO was added to the α-pinene & OH system under otherwise same chamber settings. The observed organics/SO_4^{2-} is shown in light green small triangles. ([OH], Δα-pinene and ΔCO are not shown.) Product scavenging and OH scavenging (black arows) are taking place in the presence of acidic seed aerosols as expected, since the acidity of the seed particles should not affect the gas-phase chemistry.

The red arrows are an estimate of the gain in SOA mass by isoprene that is due to condensation/acreation reactions of isoprene oxidation products on the acidic seed particles (see also Figure S4).

In Figure 1A and Figure S3 we show the AMS organic/sulfate ratio (org/SO_4^{2-}, green circles) taking out trends and fluctuations of the seed aerosol generation, which were caused by limited stability of the seed aerosol production. The SOA mass yields in Figure 1B and the analysis of the isoprene contribution to SOA in Figure S4 are based on those experiments during the steady state periods B, C, and, D, marked by black horizontal lines in Figures 1A and S3.

The (wall loss corrected) α-pinene SOA yield in period B is practically the same (within the experimental uncertainties) for acidic seed aerosols (20%) as for the neutral case (18%) (Figure 1B, columns B). This means, that the formation of α-pinene SOA itself was not significantly affected by the acidity of the seed particles.

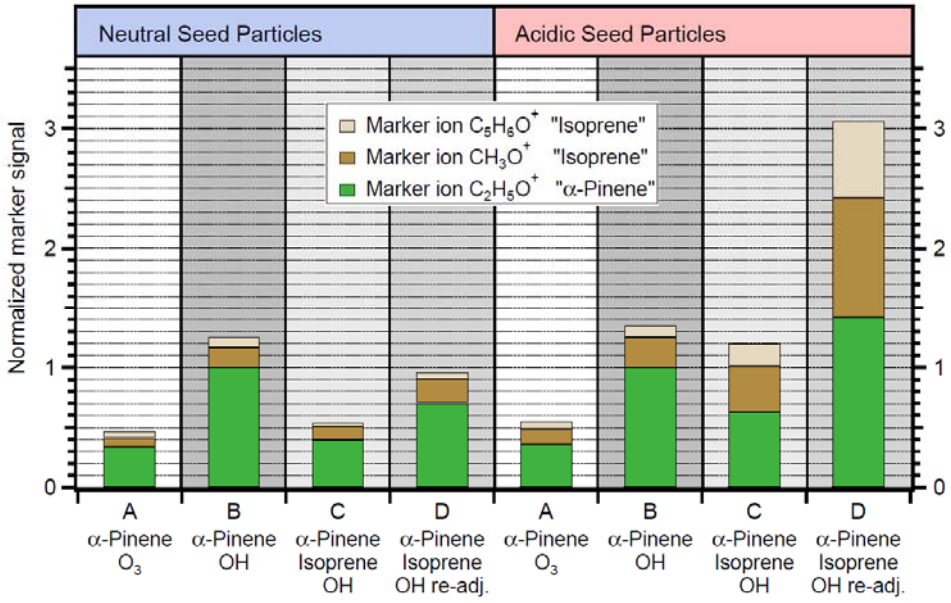

Figure S4: Isoprene oxidation products contribute to organic mass in the presence of acidic seed particles. $C_2H_5O^+$ (green) served as marker ion for the □-pinene contribution, whereas CH_3O^+ (brown) and $C_5H_6O^+$ (beige) served as marker ions for the isoprene oxidation products. All marker ion signals were normalized to $C_2H_5O^+$ during respective phase B. Note that the mass contribution of the individual marker ions to total organic mass is only of the order of percent. In the presence of **neutral seeds** (left side) $C_2H_5O^+$ followed the concentration of the total organic mass closely. Note that α-pinene oxidation products contribute somewhat to the ions CH_3O^+ (brown) and $C_5H_6O^+$(beige), but the two ions vary proportional to the $C_2H_5O^+$ ion. In the presence of **acidic seeds** (right side) the ions CH_3O^+ and $C_5H_6O^+$ showed the same low contribution in the absence of isoprene (A, B) as in the neutral case. However, both marker ions increased strongly when isoprene was added to the reaction chamber (C). They increased further when [OH] was re-adjusted (D), because of the fast reaction of isoprene with OH radicals. Clearly, isoprene oxidation products contributed to SOA mass in the acidic case. $C_2H_5O^+$ is somewhat higher in C and D compared to the neutral case, as isoprene oxidation products also contribute somewhat to the $C_2H_5O^+$ marker ion.

Addition of isoprene (red triangles) to the evolved α-pinene & OH system dropped $[OH]_{ss}$ to about 1/3 in period C (black diamonds in light grey area). The reduction of [OH] in period C has two effects: it reduced the α-pinene consumption (blue squares) thus the production of SOA mass. Moreover, the *SOA yield is lower* at lower OH due the product scavenging effect induced by the presence of isoprene (and somewhat due to OH dependence of the SOA yield in general[31,32]). The suppression of SOA mass is more distinct in presence of neutral aerosol (Figure 1A) than in presence of acidic aerosol (Figure S3). But also the *SOA yields* are reduced in both cases, by about 40% in the neutral case and by about 1/3 in the acidic case (second columns in Figure 1B). This suppression of the SOA yield we attribute to the sum of *product scavenging* and *OH scavenging* effects.

In period D (middle grey area) $[OH]_{ss}$ and thus the α-pinene consumption were re-adjusted in the presence of isoprene to the same values as observed for the α-pinene only system. As a consequence the effect of OH scavenging (marked in orange in Figures 1A and S3) is compensated. The effect is striking in the presence of neutral seed aerosol: the SOA mass remains reduced (Figure 1A) and the SOA yield is distinctively smaller when isoprene is present (Figure 1B, column D). This difference we attribute to the effect of product scavenging (marked in red in Figure 1A). As we will show in section 6, product scavenging is due to interaction of α-pinene peroxy and isoprene-induced peroxy radicals in the HOM formation process.

In the presence of acidic aerosol, the SOA mass increased after re-adjustment, however the SOA yield still remains lower. Since the acidity of the aerosols will hardly influence the gas-phase chemistry, both scavenging effects were apparently masked by isoprene oxidation products contributing to SOA mass on acidic seeds (red arrows in Figure S3). Indeed, while in case of a neutral seed aerosol we found no significant influence of SOA composition by the presence of isoprene, we directly observed the isoprene markers by aerosol mass spectrometry on the acidic seed aerosol (Figure S4) likely arising from condensed phase accretion reactions.[35-37,66,67] The suppression of α-pinene SOA is compensated by some isoprene SOA (iSOA). Nevertheless the suppression of total SOA *yield* was still recognizable in the presence of acidic seeds (Figure 1B) and even more so in Figure 2. Note that in both OH adjustment experiments (Figure 1A and Figure S3) the consumption of α-pinene and isoprene in terms of mixing ratio are quite similar. This choice was determined by the experimental boundary conditions for such complex experiments. This means that the ratio of Δisoprene/Δα-pinene in units of mass concentration is about ½ only, thus on the very left side in Figure 2. Insofar, the product scavenging effect is expected to be much larger at higher Δisoprene/Δα-pinene.

The iSOA contribution can be estimated by comparison with the SOA mass formation when isoprene is replaced by CO at otherwise same conditions (Figure S3, light green trace). In contrast to isoprene oxidation products, the CO oxidation product CO_2 cannot contribute to SOA formation. In presence of CO the OH scavenging effect and the product scavenging effect after re-adjustment of $[OH]_{ss}$ in presence of acidic aerosols in Figure S3 were strikingly similar to the effect of isoprene in presence of neutral aerosols in Figure 1A.

The strength of the compensating effect of accretion reactions of isoprene oxidation products, as indicated by the red arrows in Figure S3, is of course larger at higher $[OH]_{ss}$, thus higher isoprene consumption. A difference between isoprene and CO is that isoprene raised the level of organic peroxy radicals with ≤ 5 carbon atoms (and HO_2 radicals), while CO raised only the level of HO_2 radicals. The interaction of both types of peroxy radicals with α-pinene peroxy radicals in HOM formation are the core of the product scavenging effect.

We conclude that the *product scavenging* effect is also active in presence of acidic seed aerosols, as the gas-phase peroxy chemistry should not be affected by the acidity of the seed particles, however the effect is masked / compensated by accretion reactions of isoprene oxidation products. As we document in the main manuscript (Figure 4) and in section 5, the findings shown here for α-pinene & isoprene and α-pinene & CO demonstrate a general behavior. In further experiments we showed that CH_4 also suppresses SOA yields of α-pinene, and that isoprene also suppresses the SOA yield of β-pinene.

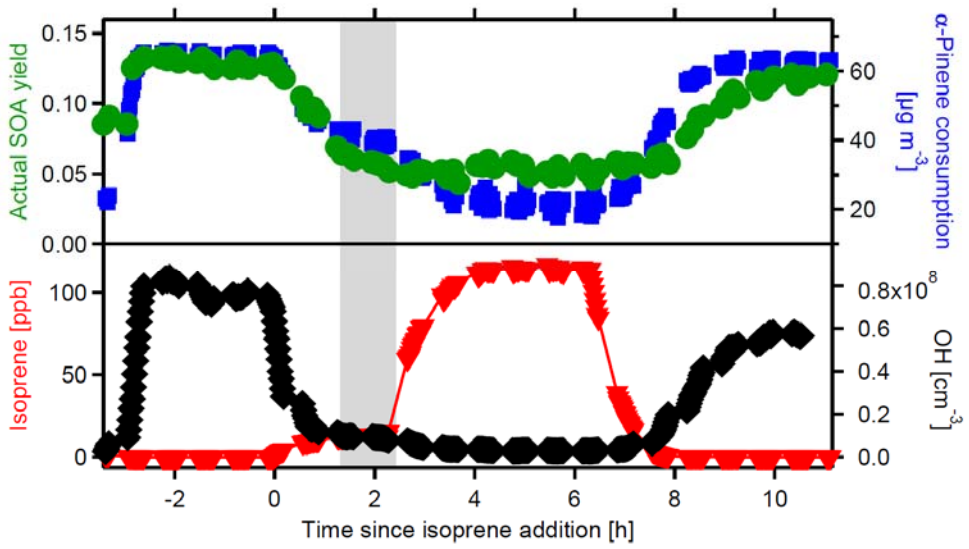

Figure S5: Product scavenging and OH scavenging in the reaction system α-pinene & isoprene & OH. The actual SOA yield, calculated as actual organic mass / actual α-pinene consumption, can serve as diagnosis of the product scavenging effect. The actual yield decreases by more than 50%, when isoprene is added to the reaction system, mainly because of product scavenging. By referring to the actual α-pinene consumption the OH scavenging through the linear mixing effect of is taken out. The grey-shaded area shows the effect at 1:1 α-pinene/isoprene ratio at chamber inlet.

5. Generality of OH and product scavenging and suppression of SOA yields.

Product scavenging is not only operative in the α-pinene & isoprene & OH system. We illustrated that already for α-pinene & CO & OH system in presence of neutral aerosols and acidic aerosols (Figures 4 and S3). As we showed in Figures 1B and 2, a necessary strong indicator for product

scavenging is a lower *actual SOA yield*. If the OH cannot be adjusted (like in Figure 1A), inspection of the actual SOA yield in presence and absence of the scavenger can still provide a diagnostic for product scavenging, since the yield is normalized to the actual precursors consumption thus takes out the part of the simple OH scavenging effect related to the linear mixing rules (section 2). The example for the α-pinene & isoprene & OH system is given in Figure S5. In the same sense product scavenging is also observed in the β-pinene & isoprene & OH system (Figure S6). Here the actual yield of β-pinene SOA is suppressed by about 40%, clearly indicating that product scavenging by isoprene is not limited to α-pinene.

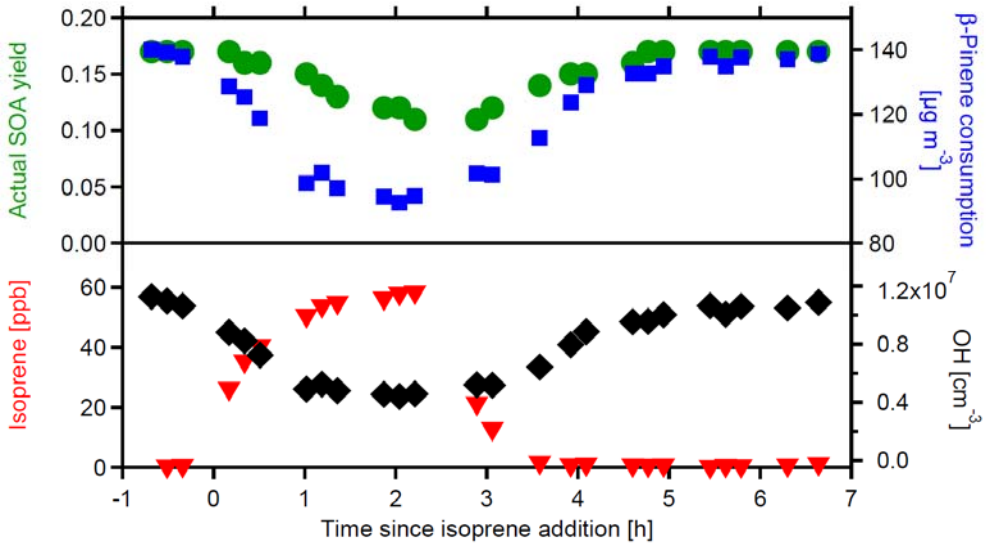

Figure S6: Product scavenging and OH scavenging effect in reaction system β-pinene & isoprene & OH. The actual SOA yield, calculated as actual organic mass / actual β-pinene consumption, decreases by 40%, when isoprene is added to the reaction system.

Also in binary mixtures of α-pinene and compounds without SOA forming potential, like CO and CH_4, a decrease of the actual α-pinene SOA yield was observed, thus product scavenging can be diagnosed. In **Figure 4**, the additions of CO (10 ppm, 57 ppm) to the α-pinene & OH system suppresses the total HOM by a factor 4-5 and the dimer fraction by more than a factor of 2 (**Figure 4A**). The actual SOA yield of α-pinene was reduced by more than 60% in the presence of 40 ppm CO.

The most abundant organic peroxy radical in the atmosphere is CH_3O_2, which is formed in the atmospheric degradation of methane CH_4 by OH. Mixing α-pinene and CH_4 in presence of acidic seed aerosols also leads to suppression of the α-pinene SOA yield (Figure S7). Note: the conditions in JPAC were forced to yield a significant consumption of methane in order to generate CH_3O_2 radicals. To estimate the possible effect of CH_4 on SOA formation under

atmospheric conditions we corrected for the too high CH_3O_2 radicals produced in our chamber. We use α-pinene as a surrogate of all MT, and the OH reactivities of CH_4 and α-pinene as estimate of the ratio of CH_3O_2 and α-pinene peroxy radicals (R_{CH4}/R_{MT}). Summer monoterpene concentrations at the SMEAR station in Hyytiälä are typically several 100 ppt[68] and CH_4 is around 1.8 ppm; R_{CH4}/R_{MT} in Hyytiälä is about 0.6 assuming 300 ppt MT. In the experiment shown in Figure S7 the ratio of CH_4 reactivity / α-pinene reactivity was ~ 2 and the yield of α-pinene was suppressed by about 50 %. If we choose the simplest approach, i.e. to scale the suppression of SOA formation with R_{CH4}/R_{MT} (= ratio of consumption), we estimate an suppression of the order of 15 %. If the CH_4 chemical system behaves in a similar manner to the isoprene system than we would expect a suppression of 16% from the parametrisation as given in Figure 2. Furthermore, at the relative constant ambient CH_4 concentrations, the relative impact of CH_4 should increase with decreasing monoterpene concentrations.

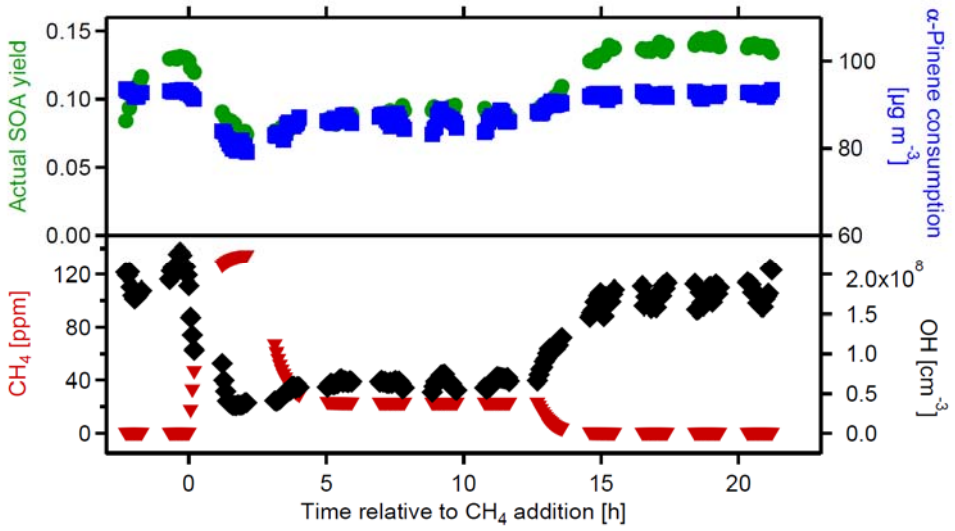

Figure S7: Product scavenging effect in reaction system α -pinene & CH_4 & OH. The actual SOA yield, calculated as actual organic mass / actual α -pinene consumption, drops, when CH_4 is added to the reaction system. CH_4 concentrations were calculated from known inlet concentration, the flow rate through the RC and the reaction rate of CH_4 with OH.

Given the generality of product scavenging, it is obvious that the SOA mass formed from a mixture cannot be approximated linearly. Calculating the SOA mass formed by oxidation of individual compounds from their individual yields and their consumption and then adding up these SOA masses will overestimate the total SOA formation. The basic mechanisms identified here show that - due to basic photochemical processes - the SOA yield of an individual compound also depends on other molecules in the respective environment.

6. Gas-Phase HOM Chemistry: Dimer Suppression

Peroxy radicals are key players in atmospheric oxidation of organic compounds. They are formed via H-abstraction by OH or addition of OH to double bonds. During ozonolysis, peroxy radicals are also formed via the vinylhydroperoxide path. In competition with termination reactions, peroxy radicals can undergo intramolecular H-shifts forming a hydroperoxide group and a carbon centered radical.[45,69,70] The latter rapidly adds air oxygen reforming the peroxy functionality. The sequence of H-shifts and O_2 addition is called autoxidation[71] and can lead to very fast formation of highly oxygenated multifunctional peroxy radicals (HOM-RO_2) with O/C up to one or even higher. HOM-RO_2 are terminated like other peroxy radicals[45] and the interplay of autoxidation and termination reactions results in stable highly oxygenated multifunctional molecules (HOM[22,45,52,70]). In our experiments at low NO concentrations HOM-RO_2 are mainly terminated by other peroxy radicals, including HO_2. HOM are compounds of low or extremely low volatility (LVOC or ELVOC)[22,39,72] and we will show that the reduction of SOA yields due to the product scavenging effect are related to changes in HOM.

In order to understand the product scavenging effect on molecular level it is important to note that in reactions between HOM-RO_2 also HOM-dimers are formed, e.g. C_{17}-C_{20}-HOM in the case of α-pinene (Figure S8)[22,38]. The O/C ratios of HOM dimers are typically lower than those of HOM monomers, and, as shown for cyclopentene and cyclohexene, dimers involve also the most abundant primary peroxy radicals[45]. The exact mechanism of the self-dimerization is yet not clear, but rates for dimer formation are high for functionalized RO_2 radicals[38], sufficiently high to compete with termination reactions with RO_2 and HO_2. From their structure and their O/C ratios dimers are organic compounds with extreme low volatility (ELVOC) [38,39,45,70,72] and HOM-monomers and HOM-dimers together can dominate SOA formation, up to 50%-100% in early phases of SOA formation.[22]

We studied the HOM *gas-phase* chemistry for α-pinene and α-pinene/isoprene mixtures by Chemical Ionization Time of flight Mass Spectrometry and could observe directly the suppression of α-pinene HOM-dimers in the presence of isoprene (see Figure 3A). This effect of isoprene becomes clear by comparing the HOM distribution in monomers and dimers at the same α-pinene turnover in Figure 3B, with the [OH] tuned by either adding different amounts of isoprene (red) or by modifying the O_3 photolysis rate $J(O^1D)$ (blue). We grouped HOM-monomers and HOM-dimers using the center of the mass spectrum envelope at m/z = 370 Th as separation criterion, and took the sum over all m/z as HOM-total. For easier comparison we normalized the data for the observations at the highest turnover where [isoprene] approached zero.

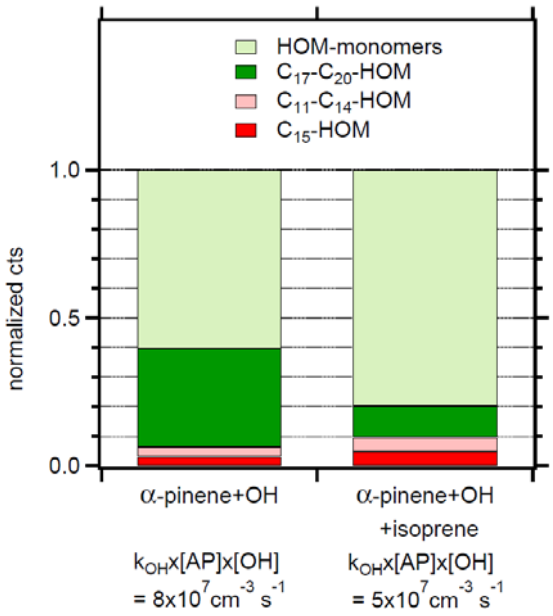

Figure S8: Relative contribution of HOM monomers, α-pinene derived C_{17}-C_{20} dimers and potentially mixed C_{11}-C_{15} dimers isoprene/α-pinene with C_{15} separated as lead mixed dimer before isoprene addition (left) and at maximum isoprene concentration (right). C_{11}-C_{15} dimers were also observed in the α-pinene only system, but only as small fraction. The drop of the C_{17}-C_{20} fraction is due to both OH and product scavenging. The fraction of C_{11}-C_{14} dimers and the lead C_{15} dimer increase somewhat in the presence of isoprene indicating that indeed mixed isoprene/α-pinene dimers are formed, but not in large amounts. The data were normalized by 344 cts (left) and 151 cts (right).

The total HOM concentration decreases more strongly when [OH] is decreased by increasing isoprene concentrations, than by decreasing the photolytic production of OH (as described in the main manuscript, Figure 3B, red and blue circles). This is mainly due to the decrease of the HOM dimer concentration, clearly decreasing more strongly with increasing isoprene than with decreasing $J(O^1D)$ (red and blue squares, respectively). Based on the molecular formulas assigned to each *m/z* in high resolution mass spectra, we weighted the signal for each compound by the molecular mass and summed up the so derived "mass concentrations" for all monomers (C≤10) and all dimers (C>10). A peak list of the attributed molecular formulas for the most prominent signals is given in Table S3a andb . For an α-pinene turnover of $5x10^7$ cm^{-3} s^{-1} (middle arrow in Figure 3B) we estimated the suppression of the HOM-dimers (dark green bars, Figure 3C). For that we scaled the mass concentrations from the α-pinene $J(O^1D)$ experiment, which was performed at a lower α-pinene inlet mixing ratio (10 ppb vs. 25 ppb) by a factor 2.3, to match the same (initial) conditions as for the α-pinene-only reference experiment for the isoprene series and then interpolated the observations at $4.3 \cdot 10^7$ cm^{-3} s^{-1} and $5.7 \cdot 10^7$ cm^{-3} s^{-1} to $5.0 \cdot 10^7$ cm^{-3} s^{-1} as indicated in Figure 3C. We estimate a drop by 33% of the total HOM mass of which 26% is due to reduced HOM-dimer concentrations and the other 7% due to HOM-monomers. Since we

compare values at the same α-pinene turnover this reflects indeed the effect of product scavenging.

Assuming that SOA is predominantly formed from HOM and that HOM-dimers are effectively non-volatile and will fully contribute to SOA mass, the 27% mass suppression of HOM dimers explains most of the overall reduction of SOA mass of about 35%, due to the product scavenging effect in Figure 1A. Note again that HOM are responsible for 50-100% of the SOA mass under these conditions and that the reduction predicted from the suppression of dimers fits the experimentally determined reduction of SOA mass quite well.

Table S3 Peak lists for α-pinene and α-pinene & isoprene mixtures

α-Pinene						
	Formula		Exact mass [m/z]	HOM [Da]	error [ppm]	rel intensity [%]
C5	C5 H6 O6		224.005	162.016	2.2	0.73
	C5 H7 O6		225.013	163.024	-1.4	0.21
	C5 H5 O7		238.992	177.004	-12.7	0.38
	C5 H6 O7		240.000	178.011	-1.3	0.31
	C5 H7 O7		241.008	179.019	-5.2	0.31
C10	C10 H16 O6		294.083	232.095	4.7	1.06
	C10 H14 O7		308.062	246.074	1.7	0.82
	C10 H16 O7		310.078	248.090	-3.6	9.58
	C10 H14 O8		324.057	262.069	5.8	1.53
	C10 H16 O8		326.073	264.085	-6.1	4.49
	C10 H14 O9		340.052	278.064	5.9	1.05
	C10 H16 O9		342.068	280.079	-9.3	1.85
	C10 H14 O10		356.047	294.059	13.1	0.78
	C10 H16 O10		358.063	296.074	-4.4	0.81
	C10 H15 O11		373.050	311.061	-10.0	0.86
	C10 H16 O7	HNO3*NO3-	373.074	248.090	-7.8	2.58
	C10 H16 O11		374.058	312.069	3.1	0.66
	C10 H14 O8	HNO3*NO3-	387.053	262.069	-4.6	1.04
	C10 H16 O8	HNO3*NO3-	389.069	264.085	-13.7	1.14
C15	C15 H22 O9		408.115	346.126	7.3	0.26
	C15 H22 O10		424.110	362.121	-8.6	0.25
	C15 H22 O11		440.105	378.116	13.8	0.6
	C15 H22 O12		456.099	394.111	-6.7	0.25
	C15 H24 O12		458.115	396.127	-1.9	0.16
C20	C20 H30 O9		476.177	414.189	-7.0	0.82
	C20 H30 O10		492.172	430.184	-9.2	0.87
	C20 H32 O10		494.188	432.200	-1.9	0.45
	C20 H30 O11		508.167	446.179	-7.6	1.52
	C20 H32 O11		510.183	448.194	-1.8	0.74
	C20 H30 O12		524.162	462.174	-8.9	0.93
	C20 H32 O12		526.178	464.189	10.0	1.09
	C20 H29 O13		539.149	477.161	3.2	0.31
	C20 H30 O13		540.157	478.169	-7.4	0.99
	C20 H30 O14		556.152	494.164	-8.8	0.49

α-Pinene + isoprene						
	Formula		Exact mass [m/z]	HOM [Da]	error [ppm]	rel intensity [%]
C5	C5 H6 O7		240.000	178.011	-1.3	0.79
	C5 H8 O8		258.010	196.022	-3.5	1.5
	C5 H10 O8		260.026	198.038	-10.9	1.61
	C5 H9 O9		275.013	213.025	2.6	0.68
	C5 H10 O9		276.021	214.032	-2.9	0.87
C10	C10 H16 O6		294.083	232.095	10.5	0.54
	C10 H14 O7		308.062	246.074	-3.9	1.33
	C10 H16 O7		310.078	248.090	-7.6	6.02
	C10 H14 O8		324.057	262.069	5.2	1.26
	C10 H16 O8		326.073	264.085	-13.0	1.5
	C10 H14 O9		340.052	278.064	13.3	1.18
	C10 H16 O9		342.068	280.079	-14.0	1.78
	C10 H14 O10		356.047	294.059	13.1	0.74
	C10 H16 O10		358.063	296.074	-4.4	0.91
	C10 H15 O7	HNO3*NO3-	372.066	247.082	6.0	0.51
	C10 H15 O11		373.050	311.061	-10.0	0.76
	C10 H16 O7	HNO3*NO3-	373.074	248.090	-7.8	1.59
	C10 H14 O8	HNO3*NO3-	387.053	262.069	-4.6	0.91
	C10 H16 O8	HNO3*NO3-	389.069	264.085	-13.7	0.52
C15	C15 H24 O10		426.125	364.137	-9.9	0.42
	C15 H26 O10		428.141	366.153	-2.7	0.49
	C15 H24 O11		442.120	380.132	-10.1	0.54
	C15 H24 O12		458.115	396.127	-1.9	0.43
	C15 H26 O13		476.126	414.137	-11.1	0.33
C20	C20 H34 O8		464.214	402.225	-3.9	0.15
	C20 H32 O9		478.193	416.205	9.3	0.14
	C20 H32 O10		494.188	432.200	1.3	0.15
	C20 H34 O10		496.204	434.215	15.6	0.15
	C20 H30 O11		508.167	446.179	-7.6	0.19
	C20 H32 O11		510.183	448.194	-1.8	0.31
	C20 H30 O12		524.162	462.174	-8.9	0.17
	C20 H32 O12		526.178	464.189	10.0	0.4
	C20 H30 O13		540.157	478.169	-7.4	0.21
	C20 H32 O13		542.173	480.184	11.0	0.16

The interaction of α-pinene HOM peroxy radicals with isoprene peroxy radicals, does not lead to significant contributions to mixed α-pinene-isoprene dimers. In Figure S8 we compare the sum of HOM-monomer concentrations with several HOM dimer-concentrations before and at the maximum of isoprene addition with α-pinene input (25 ppb) held constant. We chose C_{17}-C_{20} compounds (dark green) as lead class of α-pinene derived dimers, and C_{11}-C_{15} compounds (reddish) as lead class of potential mixed α-pinene/isoprene dimers. We also show C_{15}-HOM (red) as marker for direct C_{10}-peroxy + C_5-peroxy radical recombination. First we note that C_{11}-C_{15} dimers are also formed by α-pinene and C_{15}-HOM provides the major contribution to the C_{11}-C_{15} class. In this case C_{11}-C_{15} dimers must arise from fragmented α-pinene oxidation products. The concentration of C_{17}-C_{20} dimers (dark green) is about five times higher than C_{11}-C_{15} dimers (reddish). C_{17}-C_{20} dimers are ≈35% of the total HOM in absence of isoprene. When isoprene is

maximal, HOM monomers (light green) drop by 40%, mainly due to the OH scavenging effect by isoprene, however C_{17}-C_{20} dimers drop by ≈90% due to both OH and product scavenging effect. C_{11}-C_{15} dimers and C_{15}-HOM marker are still lower than in absence of isoprene because the isoprene induced drop in [OH] over-compensates the formation of isoprene derived C_{11}-C_{15} dimers and the C_{15}-HOM marker. The relative increase of C_{11}-C_{15} dimer fraction offsets only very little of the product scavenging effect in accordance with the observation in Figure 2A, where only weak signals were recognizable in the C_{15}-HOM *m/z* range.

We conclude that the product scavenging effect in the presence of isoprene is due to additional termination reactions of α-pinene HOM-RO_2 with isoprene RO_2 and isoprene related increased HO_2. This clearly reduces the concentration of α-pinene dimers and explains already a major portion (4/5) of the SOA mass reduction. As indicated in the mass spectrum in Figure 2A presence of isoprene shifted in addition the HOM monomers to smaller masses, thus to higher vapour pressures. Both contributions led to less HOM with extreme low vapour pressures and reduced SOA mass. Our findings are in accordance with the suggestions that HOM-dimers and only a fraction of HOM monomers are ELVOC.[25,64]

It is interesting to note that the overall HOM signal, comprising monomers and dimers, is increasing nearly linearly with the α-pinene turnover on a logarithmic scale, indicating non-linear behavior (Figure 3B). This is independent on the OH concentration being varied by different isoprene additions or by varying $J(O^1D)$. One reason is that HOM themselves are likely formed by a combination of autoxidation and sequential oxidation. The observed non-linearity with OH suggest that at least one extra oxidation step is involved of the formation of a portion of the HOM. Indeed, mass spectra of HOM derived from oxidation of pinonaldhyde by OH look very similar to those derived from a-pinene in the same way, and both are distinct from mass spectra derived from α-pinene ozonolysis. Since HOM contribute significantly to SOA, we conclude that the non-linear dependence of HOM formation on OH can explain parts of the OH dependence of the SOA yields observed for α-pinene and β-pinene (e.g.[31,32]).

Note HOM are very likely a mixture of LVOC and ELVOC from primary and secondary oxidation. A certain fraction of HOM are ELVOC (10-20%)[39] and the condensed LVOC and ELVOC provide an organic matrix for dissolution of semi-volatiles into particles. Although HOM will contribute large portions to SOA mass, this does not exclude significant contributions by products arising from classical ageing, i.e. sequential oxidation by OH[e.g.2].

7. Model study of isoprene chemistry under conditions prevailing in JPAC

The SOA yield from isoprene has been treated in numerous publications and estimates range from a few percent up to 30% illustrating the complexity of the chemistry including heterogeneous and in parts acid catalyzed condensed phase processes.[10,12,73-78] The yields of isoprene SOA (iSOA) in our experiments are on the low side of observations. Studies have shown that iSOA yields in chamber studies are sensitive to the oxidation conditions, e.g. on $[HO_2]$ and $[RO_2]$.[10,74] In the following we will present results from model calculations that show

that the key SOA precursor and HO_2 concentrations for our experimental conditions in JPAC should be either comparable or even higher than in the atmosphere. For that we will utilize box model calculations under the boundary conditions of a perfectly stirred continuous tank reactor (CSTR) for JPAC.

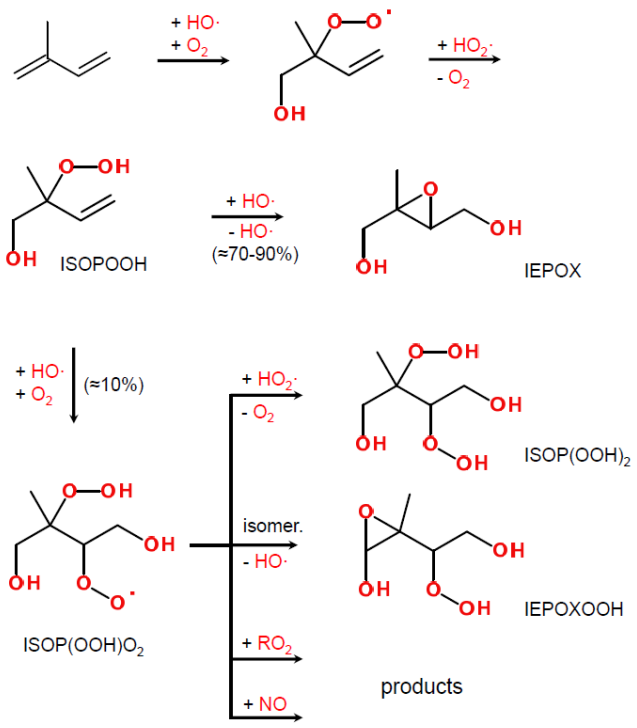

Figure S9: Exemplary reaction scheme for oxidation of isoprene by OH leading to iSOA precursors (compare[74,79,80]). Two types of iSOA precursor species are formed via ISOPOOH: IEPOX (acidic aerosols) and $ISOP(OOH)_2$ (neutral aerosols). Note: the structures depicted are just examples for a set of stereoisomers.

Figure S9 summarizes a part of the isoprene oxidation mechanism that we would like to address: isoprene is oxidized by OH addition to one of the isoprene double bonds resulting in the formation of several isomeric isoprene hydroxyl peroxy radicals OH-ISOP-O_2. These either react in the usual way with NO, HO_2, and other peroxy radicals (RO_2) or rearrange to form hydroperoxy aldehydes (HPALD) or HOM-like compounds by autoxidation.[10,41,74,79-82] At low NO_X in non-polluted areas, corresponding to the regimes that were addressed in our study, termination by HO_2 forming hydroxyl hydroperoxides (ISOPOOH) is a major pathway.

Reaction of OH with ISOPOOH occurs predominantly by addition to the remaining double bond, which has two pathways (Figure S9).[10,76,79,83] The major pathway leads to formation of isoprene epoxydiols (IEPOX) with regeneration of OH (70%-80%), while the minor pathway, after O_2 addition, leads to a dihydroxy hydroperoxy peroxy radical ($ISOP(OOH)O_2$, 10%[74,79,83]). This

complex peroxy radical can subsequently undergo bimolecular reactions with HO_2, NO, or RO_2, leading to the respective products, or undergo autoxidation via isomerisation. A significant product is the compound with O/C = 6/5 and H/C = 12/5, formed from the termination reaction with HO_2 (Figure S9), and hereafter referred to as ISOP(OOH)$_2$. IEPOX form significant amount of SOA by condensed phase chemistry on acidic aerosols but are not so important in the presence of neutral aerosols. Recent experiments starting from ISOPOOH indicate a significant build-up of SOA material in presence of neutral particles based on the dihydroxy-dihydroperoxy path and ISOP(OOH)$_2$.[10,66,74,76,79]

In order to get a hold of the peroxy radicals concentrations [HO_2] and [RO_2] as well as on the concentrations of ISOPOOH and the IEPOX SOA precursors in the gas-phase, we applied the MCM v3.3.1 mechanism adapted to JPAC which included an updated isoprene mechanism[80]. We deduced also ISOP(OOH)$_2$ and HOM, which are not included in the updated MCM v3.3.1 for isoprene, from the model calculations.

We conducted free running forward calculations varying the isoprene input concentrations over our experimental range. The intensity of the TUV lamp (254nm), thus primary ozone photolysis, was adjusted by less than 5% to reproduce the observed $[O_3]_{ss}$ in the RC. Residence time was kept fixed at 50 min for all model runs. Model calculations were performed using the model environment EASY which is an interface for the FACSIMILE solver for differential equations.[84]

Experiments with isoprene for determination of the iSOA yields were performed at two different O_3 inlet concentrations ($[O_3]_{in}$) of 110 ppb and 55 ppb in presence of neutral and acidic seeds, respectively, but otherwise at similar boundary conditions. $[O_3]_{in}$ is the only difference in the boundary conditions from the view point of the gas-phase chemistry and thus stand also for the two experimental cases neutral and acidic seeds. In addition we run an "atmospheric" case, simulating "typical" ambient actinic flux, OH and isoprene concentrations (see below).

In the model runs, the isoprene inflow was increased stepwise and for each increment the reactions system was calculated into a new steady state (model output after 6 h reaction time at 50 min residence time). The steady state model outputs were compared to the experimental observations. The observables which we compared to the model were isoprene ([C_5H_8]) in the chamber, isoprene consumption (inlet concentration - [C_5H_8]), ozone and OH. The latter was determined from the isoprene consumption.

Figure S10A and S10B show good agreement between the model and the measurements especially considering the minor adjustments applied. Deviations between the model and observation depend on uncertainties in the detailed flows delivering O_3, H_2O and isoprene to the chamber. The comparison is less convincing at the very high inlet isoprene concentrations. The model reproduces [OH] well within the experimental error of a factor of two. The other observables were satisfactorily reproduced by the model: <10% deviation for isoprene steady state concentration, and < 5% for O_3. We therefore feel confident to use the model results for [HO_2], [RO_2], IEPOX, and ISOPOOH to discuss the extrapolation of our JPAC results to atmospheric conditions.

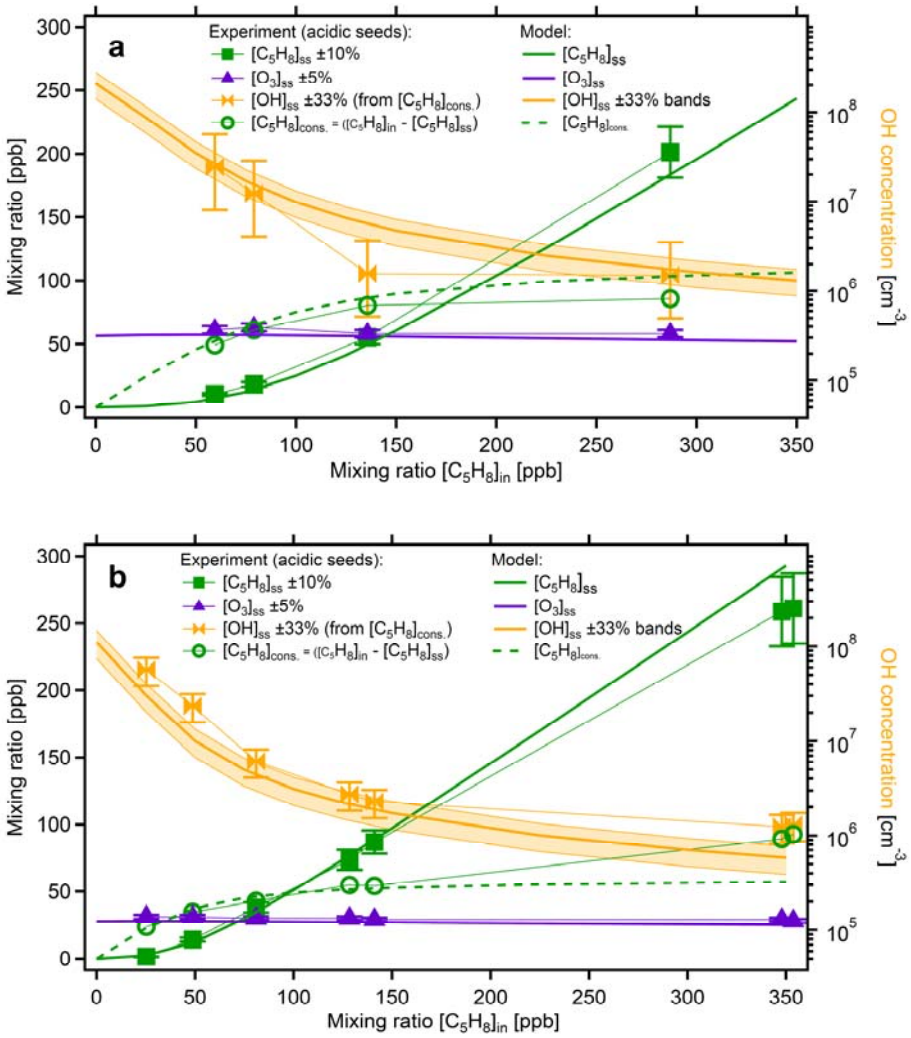

Figure S10: Comparison of model and observation for the experiments wherein the iSOA yields were determined on neutral (panel a, $[O_3]_{in}$ = 110 ppb) and acidic aerosol (panel b $[O_3]_{in}$ = 55 ppb). The steady state concentrations of OH, isoprene and O_3 are shown as a function of the isoprene inflow $[C_5H_8]_{in}$ as well as the isoprene consumption which is the difference between inlet and outlet of the reaction chamber. Each point is one steady state experiment for the given isoprene mixing ratio in the inflow.

In order to mimic the atmospheric situation in a simple fashion, we run the model for JPAC with fixed [OH] of $5x10^6$ cm^{-3}, ozone as in the acidic seed case ($[O_3]_{in}$ = 55 ppb) and at isoprene steady state concentrations in a range from 1 - 15 ppb ($[C_5H_8]_{in}$ = 2.5 - 35 ppb). The photolysis frequencies were set to 50% of noon values at the equator. The results for the so defined atmospheric case will then be compared to the corresponding model results for the experimental neutral and the acidic case.

Gas-phase concentration of key species

Under the boundary conditions where the yields for iSOA were determined [HO_2] was about $0.8 \cdot 10^{10}$ and $1.4 \cdot 10^{10}$ cm^{-3} for acidic and neutral seed simulation, respectively (Figure S11 lower panel, blue diamonds and blue triangles), thus always higher than the [HO_2] of $3\text{-}7 \cdot 10^{9}$ cm^{-3} for the simulation of atmospheric condition (blue open circles). [RO_2] (green) was less than a factor of two higher and less than a factor 3 higher for acidic (diamonds) and neutral case (triangles), respectively. The OH production is much stronger in JPAC compared to the atmosphere leading to higher OH concentrations when low concentrations of isoprene are fed to the RC. However, the input of isoprene concentrations > 100 ppb brings [OH] in the range of atmospheric concentrations (Figure S11, upper panel).

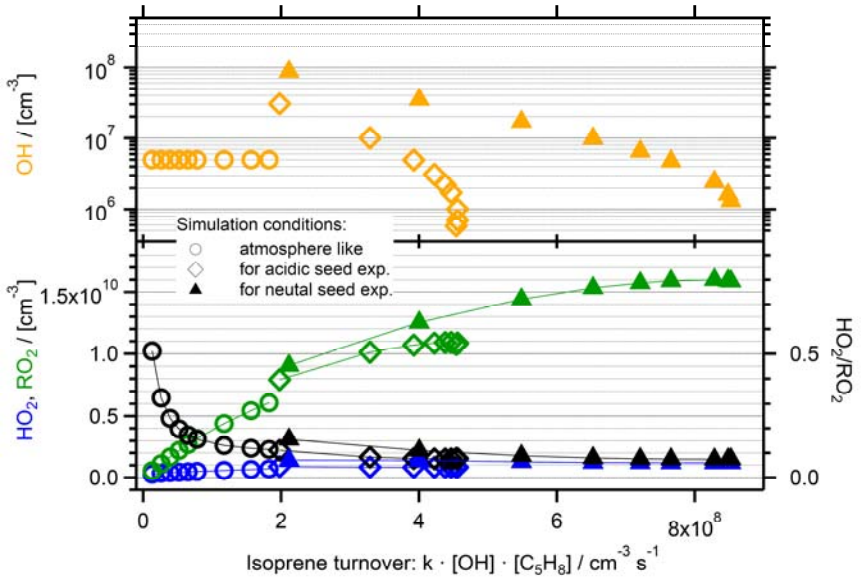

Figure S11: OH (orange, top), HO_2 (blue), RO_2 (green), HO_2/RO_2 (black, right axis) for gas-phase chemistry simulated for the JPAC conditions during the iSOA yield experiments with acidic seeds (diamonds, inlet 55 ppb O_3) and neutral seeds (triangles, inlet 110 ppb O_3). Isoprene input was varied from 25 to 350 ppb. Open circles show a simulation with OH = 5 x10^6 cm^{-3}, 55 ppb O_3 at inlet, and isoprene input ranging from 2.5 to 35 ppb (photolysis frequencies were set to 50% of the equator noon actinic flux).

Isomers of ISOPOOH are the pivotal compounds for the formation of IEPOX, $ISOP(OOH)_2$ and HOM which control iSOA formation. In the range of isoprene turnover where the iSOA yields were determined, ISOPOOH in the chamber was either about the same or up to factors of 4 or 6 higher than the maximum in the atmospheric case. Consequently, ISOPOOH concentrations were sufficiently large in the iSOA yield experiments and regarding ISOPOOH we don't expect a large bias to low iSOA yields by specific JPAC conditions.

Reasonable concentration levels of ISOPOOH and OH also guarantee reasonably high production of IEPOX, the drivers of the higher isoprene iSOA yields on acidic seed aerosols. IEPOX ranges from 6 x10^{10} cm^{-3} to 1.4 x 10^{11} cm^{-3}, which is the same as or up to a factor of two higher compared to the atmospheric simulation. In presence of neutral seeds mainly $ISOP(OOH)_2$ and isoprene HOM should contribute to iSOA, also formed from ISOPOOH via $ISOP(OOH)O_2$.[10,74,76,83] We considered the minor OH abstraction pathway (not included in MCM v3.3.1) with a branching ratio of 10%[79] (Figure S9). Applying [HO_2], [RO_2], [NO] derived in the model calculations, we calculated the branching ratio for the reactions of $ISOP(OOH)O_2$ (Figure S9). We find that the major portion (85%) leads to the functionalized epoxide IEPOXOOH, ≈10% to $ISOP(OOH)_2$, and ≈5% into the permutation reactions for the conditions of the neutral seeds. This compares to 91%, 6%, and 3%, respectively, for the atmospheric simulation. In contrast to $ISOP(OOH)_2$ the vapour pressure of IEPOXOOH is too high to condense on neutral aerosols[10,74], but it will likely undergo condensed phase reaction in acidic seeds, as other IEPOX. $ISOP(OOH)_2$ molar yields are estimated to 1% under JPAC conditions compared to 0.5% for the atmospheric simulation.

As an alternative to $ISOP(OOH)_2$ we calculated an "MCM v3.3.1 surrogate" of the total isoprene HOM concentration, for which we summed up all model compounds with O/C ≥ 6/5 in the reaction scheme. These HOM predicted by MCM v3.3.1 were maximal ≈1x10^9 cm^{-3} for the atmospheric case, and maximal ≈7x10^9 cm^{-3} for the experiment conditions with neutral seeds. The predicted HOM concentrations compare well with the estimated values for the $ISOP(OOH)_2$ channel of about 1-2.5x10^9 cm^{-3} for the atmospheric case and of ≈0.5-1.5 x 10^{10} cm^{-3} for the neutral seed case.

In summary, iSOA yields in JPAC are not biased to too low values because of too low concentrations of the major iSOA precursors for neutral ($ISOP(OOH)_2$, HOM) or acidic seeds (IEPOX, IEPOXOOH). JPAC conditions are closer to atmosphere than for example the ISOPOOH experiments which start from 60 ppb of ISOPOOH.[76] The JPAC chemical system is shifted towards RO_2, but sufficient HO_2 - more than under atmospheric conditions - is available to provide sufficient ISOPOOH and thereby IEPOX as well as $ISOP(OOH)O_2$ and $ISOP(OOH)_2$.

Mass yields of key compounds and SOA formation potential

To assess the iSOA yields we converted the modelled gas-phase concentrations of the key compounds into gas-phase mass yields and compare them to the observed iSOA mass yields listed in Table S2 (Figure S12). Gas-phase mass yields of "SOA forming compounds" can be considered as maximal "potential" for iSOA formation wherein we will use the IEPOX mass yields to represent the iSOA formation potential for acidic seeds and the $ISOP(OOH)_2$ or HOM mass yields the iSOA formation potential for neutral seeds.

For the acidic seeds case we first note that the observed iSOA yields decrease with increasing isoprene consumption, just as the modelled IEPOX yield (Figure S12, upper panel). The experiments and the model result would be fully commensurable if 15-20% of gas-phase IEPOX eventually gets transferred to the seed particles. The reaction time in the RC is about one hour and that could be insufficient to generate the iSOA mass by liquid phase processes as observed

by other groups.[8,35,74,85] However, the iSOA IEPOX yields of 15-20% compare well with observed yields in a range from a few % up to10%,[12,85,86] if one takes into account that other gas-phase compounds may also have contributed to iSOA mass (e.g. IEPOXOOH, $ISOP(OOH)_2$, HOM). Wall loss effects on the yields are small since they have to compete with the condensation on the seed particles. The yields for iSOA on acidic aerosol in Figure S12 were wall loss corrected (see Table S2). As we will show below, our iSOA yield on acidic seeds of 4% leads to about same global burden of iSOA (37%) as MT-SOA (40%, excluding NO_3-SOA contributions for both isoprene and MT) in our global model calculations in reasonable agreement with field observations (Table S5).

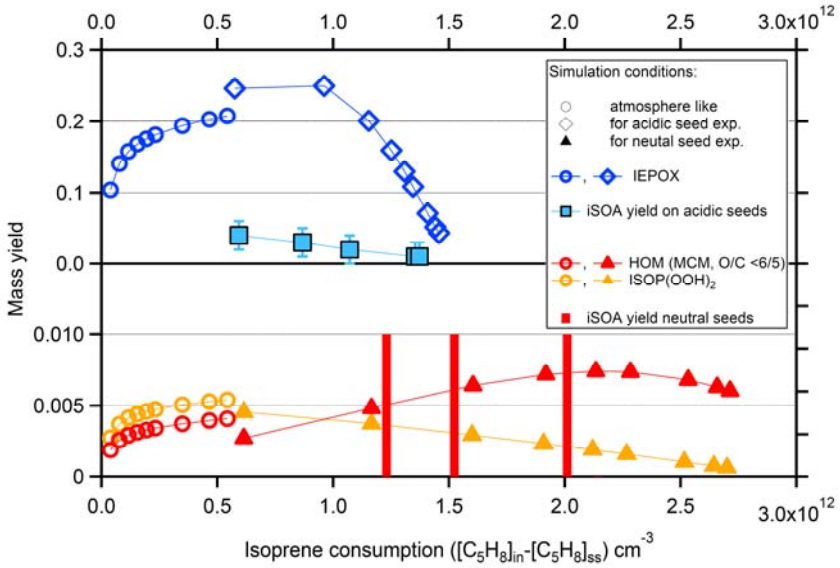

Figure S12: Comparison of the observed iSOA mass yields to the gas-phase mass yields of the major SOA-forming species IEPOX (blue, upper panel) for acidic seed, and isopene HOM (red, lower panel) and $ISOP(OOH)_2$ (orange) for neutral seed. For HOM we used two approaches, direct HOM in MCM (i.e. 9 compounds with O/C $\geq$ 6/5) and the result of an 1% branching to $ISOP(OOH)_2$ in the ISOPOOH + OH reaction, as proposed by D'Ambro et al.[66] Atmosphere like refers to [OH], [isoprene], and J values as defined in text. Gas phase mass yield can be considered as maximum "potential" of SOA formation by SOA-forming species.

In the neutral seed aerosol case the observed upper limit of the iSOA mass yield of 1% was in agreement with the estimate for $ISOP(OOH)_2$ or the prediction of HOM compounds by the actual MCM v3.3.1 mechanism (9 compounds with O/C $\geq$ 6/5). Note that we also observe only very minor isoprene HOM formation in our isoprene gas-phase experiments. However, the mass yield of ISOPOOH, and thus $ISOP(OOH)_2$ is decreasing with increasing consumption (decreasing [OH], Figure S11), while iSOA yields remained about stable. Recently, non-IEPOX pathways where described with mass yields of 4-15% at similar conditions.[10] At the moment we have no explanation for being closer to the low percentage values observed in previous studies.[75,77,87,88]

Overall we conclude that the concentrations of key species involved in iSOA formation in JPAC were commensurable with, or higher than, expectations for atmospheric conditions. To test our

findings we implemented SOA yields as determined in JPAC in the EMEP MSC-W model (next section 8).

8. Global modelling

The impact of OH scavenging and product scavenging is not limited to the α-pinene & isoprene system as we showed above (section 5). Our laboratory studies were necessarily conducted at concentration levels deviating from those in the atmosphere. Additionally, transport and dilution of emission plumes were absent under the controlled laboratory conditions. We have shown that the concentrations of the main drivers in the isoprene SOA (iSOA) formation were not too far from typical atmospheric conditions in our experiments (previous section 7). In this section we will demonstrate by global modelling studies that OH scavenging and product scavenging can play a significant role under atmospheric conditions.

Table S4: Relevant SOA yields entering the global model calculations

SOA	**Fixed yields (FY)**	**References**
MT-OH-SOA	17%	JPAC, α-pinene, for all MT, Table S1
MT-O_3-SOA	17%	JPAC, α-pinene, for all MT, derived from the seeded dark experiments
MT-NO_3-SOA	0% for α -pinene 30% for other MT	Fry et al.[102]
SQT-SOA	17%	Mentel et al.[103]
iSOA acidic seeds neutral seeds	 4% (**HI**) 1% (**LI**)	JPAC, upper limits, Table S2
	Variable yields (VY)	
MT-OH-SOA	parametrised product scavenging	JPAC, α-pinene for all MT, Figure 2

Here we focus on SOA formed by monoterpenes oxidized by OH (MT-OH-SOA). This SOA-production will respond directly to the OH scavenging and product scavenging that we have observed in the laboratory. In order to investigate the implications of these processes in the atmosphere we made use of the EMEP MSC-W chemical transport model v.4.13,[43,44,89] configured for global simulations and with a new SOA scheme for this study based on observed JPAC-yields where available (see Table S4). The gas-phase chemistry scheme used in the global modelling is based on an updated version of the CRI v2.5 mechanism[90] but with the isoprene chemistry replaced by a recently developed reaction scheme that describes the HOx recycling

mechanism (included in MCM v3.3.1) in a simplified, but acceptable, way. The rates and products of the reactions in CRI v2.5 have been reviewed and updated to take into account new and revised IUPAC recommendations, and to be in line with MCM v3.3.1. For anthropogenic organic aerosols (OA) we use a simplified framework assuming non-volatile primary OA emissions (and no additional IVOC-emissions). SOA yields from aromatic VOC oxidation were adapted from Hodzic and co-workers.[91]

Because of very large uncertainties in SOA formation itself (e.g.[1]) and varying SOA representations in regional and global atmospheric models (e.g.[92]), we limit ourselves to demonstrating that OH scavenging and product scavenging can play a role in the real atmosphere under realistic conditions of transport, dilution and varying BVOC emissions. To comprehensively and robustly quantify the importance of OH-and product scavenging for the total biogenic SOA, it would be necessary to know for certain the fraction of all major BSOA components including those formed by the two other major oxidants in the atmosphere, O_3 (MT-O_3-SOA) and NO_3 (MT-NO_3-SOA). These fractions vary from model to model depending on the photochemical scheme, SOA yields, the condensation scheme etc. Moreover, since formation of MT-O_3-SOA, SQT-SOA and even MT-NO_3-SOA may also involve autoxidation as a major process, product scavenging may also lower the BSOA mass from these components. For this reason we consider our model approach as conservative. An additional large source of uncertainty lies in the BVOC emissions.[93-96]

The EMEP MSC-W model was run for 4% iSOA yield (HI) and 1% iSOA yield (LI) using three different model configurations – denoted 'NoIso', 'FY', and 'VY'. The NoIso run represents a reference case where the model was run with fixed SOA yields as given in Table S4, and with biogenic isoprene emissions switched off. The magnitude of the OH scavenging effect by isoprene was investigated in model runs with fixed yields (FY) for all SOA types including iSOA. This FY case represents the common assumption that SOA precursors do not interact chemically with each other and that production of SOA is additive. Finally, the product scavenging effect was considered by applying variable MT-OH-SOA yields (VY), depending on the instantaneous and local isoprene/MT consumption-ratio. The product scavenging considers that the presence of isoprene lowers the fraction of condensable HOM (LVOC and ELVOC) which can be formed from α-pinene (and indeed all MT). In order to maintain consistency between the model representation of the product scavenging effect and the JPAC observations, we implemented a parametrization based upon the observed relationship between relative yield and isoprene-to-monoterpene consumption ratios (Figure 2).

In order to evaluate the performance of the revised EMEP model with the implementations we have compared its predictions of organic aerosol against two well-established monitoring networks. Firstly, for Europe, we have used data from the EMEP monitoring network (www.emep.int[97]). These data, consist of either daily or weekly samples of organic carbon (OC), measured using a mixture of PM_{10} and $PM_{2.5}$ filters. For the USA we have made use of OC data (in $PM_{2.5}$) from the IMPROVE network (http://views.cira.colostate.edu/improve[98]). These two networks provide good quality data at rural sites across the respective regions. As we are

interested in the impacts of BVOC emissions, we here consider only data from the summertime period (Apr-Sep). To avoid mountain sites we restrict the analysis to sites with altitude < 500 m. Results for the HIFY and HIVY cases were almost identical, so we present only the HIVY case here.

Figure S13 compares the summertime OC results from both networks. For Europe (Figure S13a), the model shows a good correlation with the measurement sites (R=0.64), though under-predicts by a factor of about 2 for the more polluted sites. For the USA (Figure S13b) the match between modelled and observed OC is remarkably good, with R=0.84 and almost a 1:1 relationship. Given the significant difficulties usually seen when comparing modelled versus observed carbonaceous aerosol (e.g.[92]), driven by uncertainties in precursor emissions, formation and loss mechanisms, these results are very satisfactory, and provide some confidence that the SOA yields used in this study are broadly consistent with atmospheric conditions.

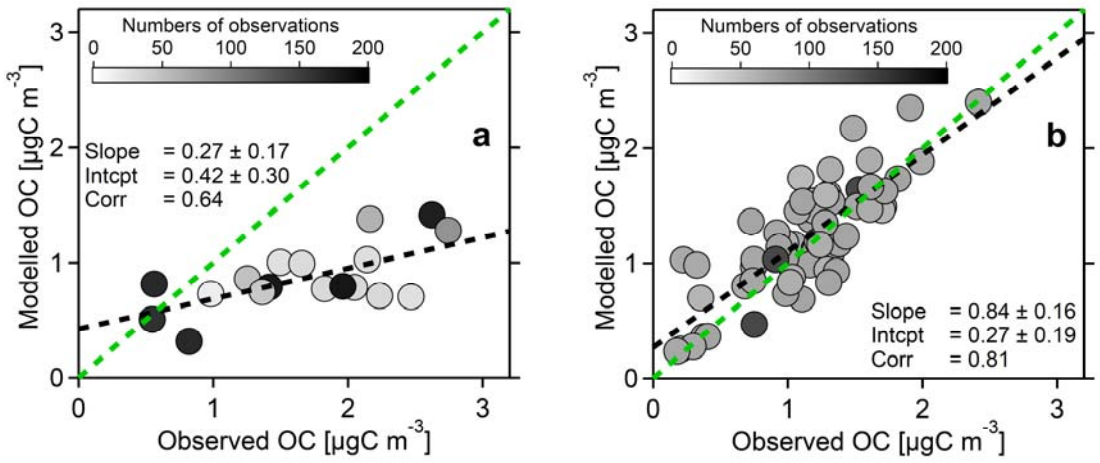

Figure S13: Comparison of modelled versus observed OC concentrations in Europe (panel a) and USA (panel b). Modelled data are from the 'HIVY' setup. European data are from the EMEP network, USA data from the IMPROVE network, see text. Data are averages from April-Sept. 2012, for sites below 500m altitude. The grey shading indicates the number of observations that were included in the comparison for the individual sites. The 1:1 line is given in green.

Table S5 shows that in the HIFY case MT-OH-SOA contributed about 20% to both the total BSOA burden (mass) and the BSOA concentration in the lowest model layer. In the surface layer the model simulated contributions to BSOA were fairly similar (15-24%) for the five classes: MT-OH-SOA, MT-O_3-SOA, MT-NO_3-SOA, iSOA and SQT-SOA.

Consistent with our JPAC experiments, inclusion of isoprene (emissions) in the model calculations substantially lowers the OH concentration (Figure S14, top). The effect is most evident in regions of high isoprene emissions such as the tropical forests in South America and

Africa. This shows that isoprene is co-controlling the available OH (compare[19]) and OH scavenging by isoprene could indeed be a substantial factor influencing MT oxidation and subsequent BSOA formation in the tropics. However, as can be also seen in Figure S14 (top), some regions exist where isoprene emissions lead to substantial increases in the modelled OH concentrations, most notably in large parts of eastern China and some areas in North America – the common feature of these regions seems to be high NOx concentrations in combination with relatively low to moderate isoprene levels in the model simulations.

Table S5: Detailed fractions of biogenic SOA on global scale

SOA fractions (FY)	Global Burden	Global Surface Concentration
MT-OH-SOA	21%	20%
MT-O_3-SOA	19%	24%
iSOA (yield 4%)	37%	24%
MT-NO_3-SOA	11%	16%
i-NO_3-SOA	3%	2%
SQT-SOA	9%	15%

The lower OH concentrations caused by isoprene *OH scavenging* are reflected in the strong decreases in MT-OH-SOA shown in Figure S14 (middle). Note, that only the linear mixing effect according Eq. 5 is considered in a fixed yield approach. A dependence of the yield on OH itself and the impact of gas/particle partitioning of semi-volatile OC (Raoult's Law effect) would further decrease MT-OH-SOA. Again the OH scavenging effect is strongest in the tropical regions, with a MT-OH-SOA reduction by 40% in South America (Figure 5). The effect should be most important in areas with sufficiently strong MT emissions in the presence of isoprene emissions. The difference plot shows that these conditions are found in tropical regions, but some effect is also seen in a wide range of temperate regions in the Northern Hemisphere (Figure S14, bottom). We conclude that OH scavenging by isoprene should lead to reduced formation of MT-OH-SOA also in a world with varying emissions, realistic isoprene/BVOC ratios, transport and dilution. On a global scale the model calculations predict surface-layer MT-OH-SOA decreases by 25% due to isoprene (Figure 5; Global). The OH scavenging effect is largest in regions with high isoprene emissions, whether densely populated (South East Asia, North America) or not (South America, South Africa). The effect is smaller in regions with low isoprene emission such as Russia and Western Europe.

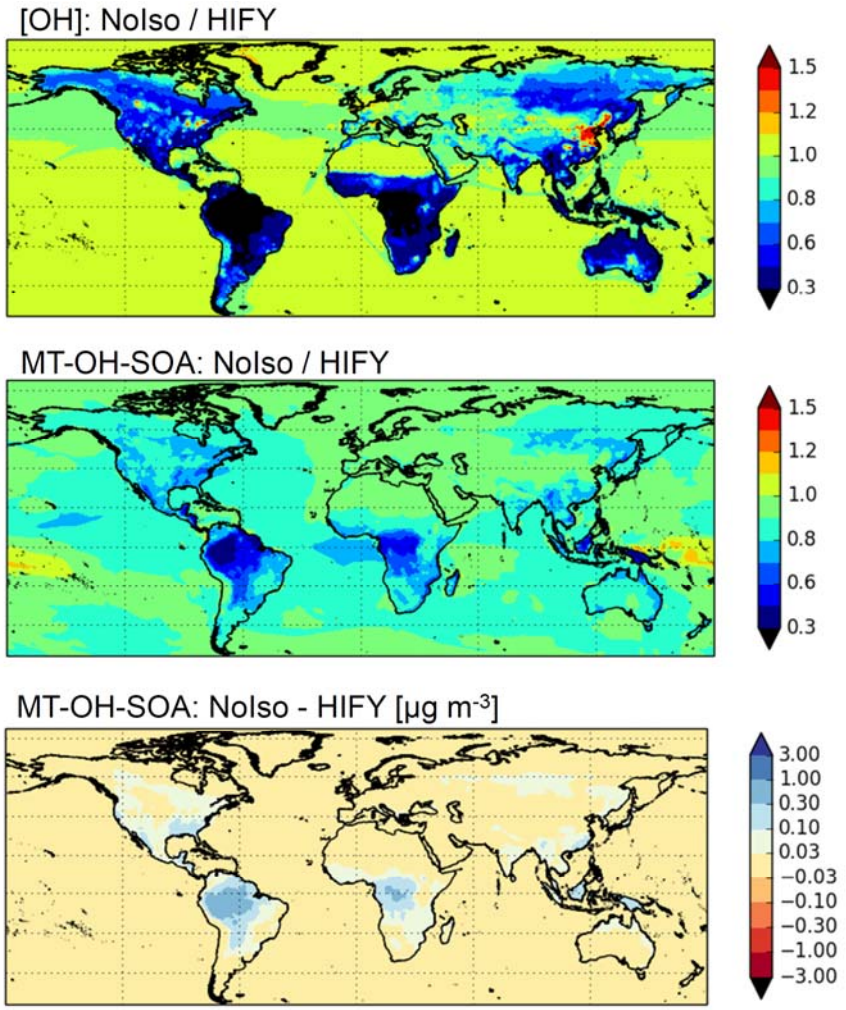

Figure S14: Effect of OH scavenging on MT-OH-SOA. Top: Ratio of the OH concentration in a world without (NoIso) and with isoprene (HIFY). Middle: Lower OH concentrations in the presence of isoprene emissions indeed reduce the MT-OH-SOA mass concentration significantly. Bottom: without OH scavenging effect by isoprene the MT-OH-SOA would be larger by up to 1 µg/m^3 in tropical regions and in the South East USA and up to 0.1 µg/m^3 in wide temperate areas (lower panel).

MT-OH-SOA is even further reduced when the *product scavenging effect* is implemented in the model (HIVY). Product scavenging reduces MT-OH-SOA (HIFY) predictions further by 10%-30% in most regions of the world; over the isoprene emitting tropical forests in South America and Africa the reduction can be >50% (Figure S15, top).

The modelled total effect of OH scavenging and product scavenging by isoprene is a reduction of MT-OH-SOA by 40% on the global scale (Figure 5). The scavenging effect is largest in regions with high isoprene/MT like South America with a reduction of 55% and South East Asia (45%)

and smaller in regions with lower isoperene/MT like Russia and Western Europe with reductions of 28% and 19%, respectively (Figure 5).

It should be noted that OH scavenging by isoprene increases the importance of MT-O_3-SOA (Figure 5, orange). The increase of the MT-O_3-SOA compensates the OH scavenging effect to some extent when the sum of MT-OH-SOA and MT-O_3-SOA (= MT-Ox-SOA, sum of red and orange bars in Figure 5) is considered. However, the reduction of MT-OH-SOA due to product scavenging still leads to significant (up to 20%) reductions of the total MT-Ox-SOA over large regions despite the compensating formation of MT-O_3-SOA (blue areas Figure S15, bottom).

Our approach is conservative. We note, that in the model calculation the iSOA production is larger than the OH scavenging and product scavenging effects for an iSOA yield of 4 %, which assumes acidic aerosol everywhere (Figure 5, sum of brownish bars). If the iSOA is formed at 1% yield (neutral aerosols) the net effect of the isoprene emissions on BSOA concentrations may even be negative in some regions (Figure 5, Western Europe).

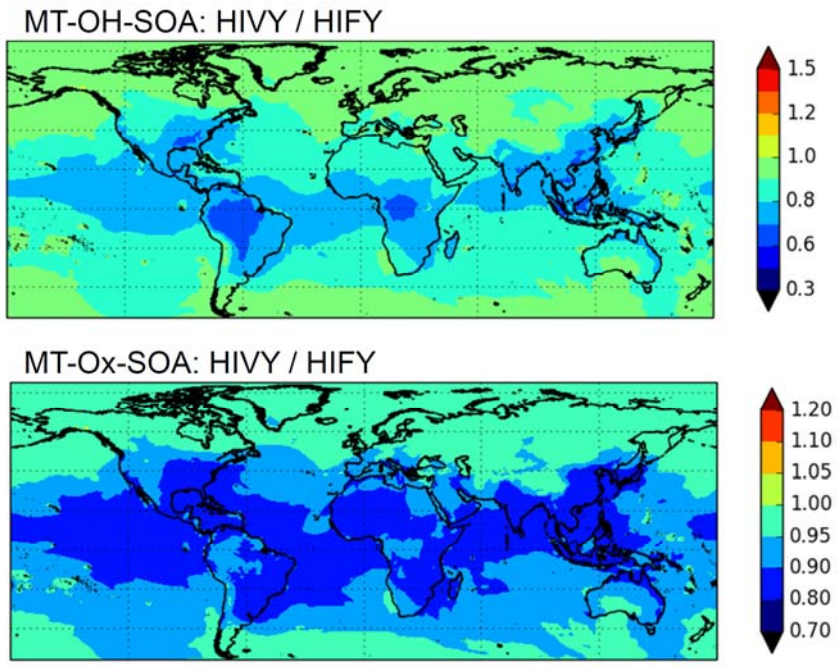

Figure S15: Effect of product scavenging as determined in this study on MT-OH-SOA (top) and on MT-Ox-SOA = MT-OH-SOA + MT-O_3-SOA (bottom).The increase in MT-O_3-SOA is not sufficient to compensate the reduction of MT-OH-SOA by the product scavenging effect.

We further note that e.g. MT-O_3-SOA also has a significant contribution of autoxidation products including HOM monomers and dimers.[22] During daytime isoprene could reduce the MT-O_3-SOA production by scavenging HOM peroxy radicals from MT ozonolysis. If we assume a similar reduction, the compensation effect by MT-O_3-SOA would be reduced. Assuming an additional product scavenging effect for MT-O_3-SOA as for MT-OH-SOA and applying the low iSOA yield (1%) would already lead to a (small) net reduction of the BSOA mass (PSOx, Figure 5). The same arguments may also hold for HOM-peroxy radicals from SQT (ozonolysis and reaction by OH) and SQT-SOA.

In summary, the model calculations clearly suggest that the OH scavenging effect (by isoprene) is significant in the real environment. The product scavenging leads to an additional substantial reduction of the MT-OH-SOA fraction. The reduction is still significant when all MT-Ox-SOA is considered although the OH scavenging effect is partly compensated by a gain in MT-O_3-SOA. To assess the overall importance of OH scavenging and product scavenging, we must assess the ratio of MT-OH-SOA to all other BSOA-components and the product scavenging in day time ozonolysis (MT-O_3-SOA) and NO_3 reactions (MT-NO_3-SOA) in the night. However, the impact of product scavenging on MT-O_3-SOA and MT-NO_3-SOA has not been determined yet and overall SOA-yields and model implementations for SOA vary widely[92] and currently we are not able to estimate the different SOA fractions with sufficient accuracy.

9. Wall effects

Wall loss in simulation chambers is currently heavily debated.[22,31,27-30] Note that JPAC is a continuously stirred flow reactor made of borosilicate glass, operated with residence times of about 50 min (Volume 1450 L, Flow 30 L/min). A fan ensures fast mixing (minute) and as a consequence the core of the reactor is always well mixed despite the losses to the walls which occur by diffusion through the laminar boundary layer near the walls. Diffusive loss is mass and size dependent and thus different for HOM monomers, HOM dimers, and aerosol particles. Details of the wall losses of HOM were described previously.[22,31] In short: chamber lifetimes of photochemically generated HOM with very low vapour pressures were determined by measuring their decay rate in the chamber after the UV-light and thus the OH production was turned off. Typically, decay rates were first order and lifetimes were of the order of 10^2 s for HOM compared to 10 min for particles with diameters of 1.5 - 7 nm[99] and 50 min for larger particles with 60-70 nm diameters. The lifetimes of the latter are similar to the residence time in the chamber, i.e. they are mainly flushed out.[46] From the determination of lifetimes for HOM in the particle free chamber we derive the set of wall loss coefficients Lw_{HOM} for individual HOM.

In the presence of aerosol particles, either photochemically produced by new particle formation or by adding seed aerosols to the chamber, condensation of HOM onto particle surfaces competes with the wall losses. Due to the additional loss of HOM by condensation to particles with coefficient Lp_{HOM} the presence of particles shortens the lifetime of gaseous HOM(g) in the chamber (Eq. 6).

$$\tau_{HOM} = \frac{1}{L_{HOM}} = \frac{1}{Lw_{HOM} + Lp_{HOM}} \quad (6)$$

With increasing particle surface, condensation onto particles competes more and more with the wall losses and eventually most of the HOM condense on particles and form SOA. The latter is the desired situation for determining SOA mass and SOA yields. For example, the lifetime of the HOM $C_{10}H_{16}O_7$ decreases in presence of increasing amount of particles, i.e. increasing particle surface from 150 s in the particle free chamber to about 20 s at a surface density of $5x10^{-4}$ m^2/m^3 (Figure S16). $C_{10}H_{16}O_7$ and the particles were generated by photooxidation experiments with increasing amounts of α-pinene. Surface densities were calculated from measurements of the number size distribution by the SMPS. $C_{10}H_{16}O_7$ is one of the largest signals in the mass spectra and as for the wall losses in the particle free chamber, the lifetime of $C_{10}H_{16}O_7$ was determined directly from the decay rate of $C_{10}H_{16}O_7$ after switching off the UV source and thus OH. Such direct measurements of lifetimes required time resolutions <10 s and many HOM signals were too weak to allow reliable determinations of decay rates at such time resolution.

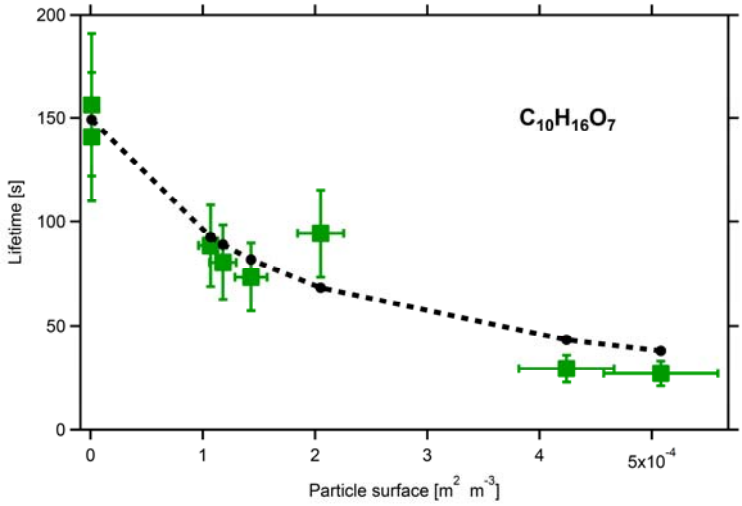

Figure S16: Lifetimes of $C_{10}H_{16}O_7$ as a function of increasing particle surface. Particles were produced by photooxidation of α-pinene at different α-pinene concentrations. The $C_{10}H_{16}O_7$ is a HOM product of α-pinene photooxidation. The lifetime was determined by analysing the decay rates of the signal of $C_{10}H_{16}O_7$ when the UV source, i.e. the OH source, was switched off. Errors of lifetimes were estimated to ±20 %, those of particle surfaces to ±10%. The dashed black line shows the life times calculated by eq. 6 with Lw_{HOM} = 1/150 s^{-1} and eq. 13 with γ=1, f_{FS}=1, and $\bar{\upsilon}$ = 156 m/s)

We therefore applied measurements at steady state conditions with increasing amount of ammonium seed aerosols allowing for the integration of HOM signals over several minutes. In steady state the concentration of a HOM, c_{HOM}, is given by the gas-phase production rate of HOM P_{HOM} divided by the total loss coefficient of HOM L_{HOM} - or multiplied by the lifetime of HOM τ_{HOM} in the chamber (Eq. 7). P_{HOM} was held constant by keeping the concentrations of the

VOC, O_3 and OH constant. L_{HOM} which is given by the sum of loss coefficients for wall losses Lw_{HOM} (neglecting the loss by flush out) and for condensation onto particles Lp_{HOM}, was varied by adding different amounts of seed aerosols.

$$C_{HOM} = \frac{P_{HOM}}{Lw_{HOM}+Lp_{HOM}} = P_{HOM} \cdot \tau_{HOM} \quad (7)$$

We normalize the experiments with seed aerosols to the case of the particle free chamber at otherwise the same boundary conditions (indicated by superscript 0); c_{HOM}/c_{HOM}^0 is then given by Eq. 8, wherein P_{HOM} cancelled out.

$$\frac{c_{HOM}}{c_{HOM}^0} = \frac{\tau_{HOM}}{\tau_{HOM}^0} = \frac{Lw_{HOM}}{Lw_{HOM}+Lp_{HOM}} \quad (8)$$

Since we are far away from saturating our mass spectrometric signals, the signal intensity is directly proportional to the concentration of the respective HOM allowing for replacing c_{HOM} by $\alpha \cdot S_{HOM}$ wherein S_{HOM} is the signal intensity measured for a given HOM and α is the respective calibration factor of the NO_3^--CIMS. In replacing c_{HOM} by $\alpha \cdot S_{HOM}$ we achieve Eq. 9 wherein the calibration factor α cancelled out.

$$\frac{S_{HOM}}{S_{HOM}^0} = \frac{Lw_{HOM}}{Lw_{HOM}+Lp_{HOM}} \quad (9)$$

Note S_{HOM}/S_{HOM}^0 is just the branching ratio into wall loss, i.e. gives the fraction of a HOM which sticks onto the wall.

We can now determine the loss to particles from the determination of Lw_{HOM} and the signal ratio S_{HOM}^0/S_{HOM} for given total particle surface S_{tot} (Eq. 10).

$$Lp_{HOM} = \frac{S_{HOM}^0}{S_{HOM}} \cdot Lw_{HOM} - Lw_{HOM} \quad (10)$$

The branching ratio into condensation i.e. the fraction of HOM (Fp_{HOM}) that form SOA is then given by Eq. 11.

$$Fp_{HOM} = \frac{Lp_{HOM}}{Lw_{HOM}+Lp_{HOM}} = 1 - \frac{S_{HOM}}{S_{HOM}^0} \quad (11)$$

As Lp_{HOM} depends on the actual particle surface, Fp_{HOM} also depends on the actual particle surface. At negligible small particle surface ($Lw_{HOM} >> Lp_{HOM}$) all HOM are lost on the walls of our chamber. At high particle surface ($Lp_{HOM} >> Lw_{HOM}$) losses of HOM on the chamber walls would be negligible.

Eq. 11 is valid for each individual HOM and for the total effect one would have to integrate over all HOM. However, in the following we will show that Fp_{HOM} will give a general correction function independent of the individual HOM. Moreover, it is valid for low volatility HOM (LVOC-HOM) if we assume that -cum grano salis - the same organic matrix is formed on the glass walls of the reactor and on the surface of seed particles. Note in this context that α-pinene SOA forms films on the surface even of aqueous ammonium sulfate seed aerosols,[100] i.e. indeed a two phase system with a separated organic phase.

Lw_{HOM} is governed by diffusion through a stagnant boundary layer at the chamber walls. Lw_{HOM} is thus proportional to the diffusion constant of HOM Dg_{HOM} and the inner surface area of the chamber Sw (7.08 m^2) and inverse proportional to the thickness (l) of the diffusive boundary layer (eq.12).

$$Lw_{HOM} = \gamma \cdot \frac{Dg_{HOM}}{l} \cdot Sw \qquad (12)$$

In Eq. 12 Dg_{HOM} is proportional to the mean molecular speed $\bar{\upsilon}$ and the mean free path λ_{HOM}. The uptake coefficient γ accounts for the fact that not every collision with the surface leads to uptake at the walls or particles (see below). Transport to the particle surface is eventually also a diffusive process. The Lp_{HOM} can be approximately described by the collisions of HOM with the total particle surface Sp_{tot} (Eq. 13).

$$LP_{HOM} = \gamma \cdot f_{FS} \cdot \frac{\bar{\upsilon}}{4} \cdot Sp_{tot} \qquad (13)$$

In Eq. 13 f_{FS} is the Fuchs-Sutugin factor[101], which is a function of the ratio of λ_{HOM} and the particle radius and interpolates between the two boundary conditions *gas-kinetic regime* and *continuous diffusion regime*. We calculated f_{FS} to be always larger than 0.85 for our experimental conditions.

Let us assume that in steady state we indeed formed the same organic matrix in particles and on the walls, which means that γ is same for both processes. The only specific molecular property in Eq. 11 and Eq. 12 is then the $\bar{\upsilon}$ which depends on the square root of the inverse molecular weight. However, $\bar{\upsilon}$ cancels out in Eq. 11 and thus Fp_{HOM} will be the same for each HOM.

We verified our approach by measuring the formed SOA mass by AMS in seeded experiments. SOA mass generated from α-pinene or β-pinene under different reaction regimes (NO_X) shows the same functional dependence on the surface of the seed aerosol (Figure S16). If we assume that SOA is essentially formed by HOM which are ELVOC, we can neglect evaporation from the walls and particles with respect to the chemical production and calculate the fraction condensing onto particles (compared to fraction sticking to the walls by Eq. 12). Fp_{HOM} was calculated by using $Lw_{HOM} = 1/\tau_{HOM}$ and Eq. 13 with $\gamma=1$ and $f_{FS}=1$ in the chamber. Fp_{HOM} curve is shown in Figure S17, it matches functionality of the observations very well. Moreover, dividing the observed organic mass by Fp_{HOM} will correct exactly for the SOA mass which was deposit on the walls. We conclude that our method of wall loss corrections is based on fundamental principles and we can reduce it to direct observations, i.e. the ratio of S_{HOM}/S_{HOM}^0 in the particle loaded and particle free chamber.

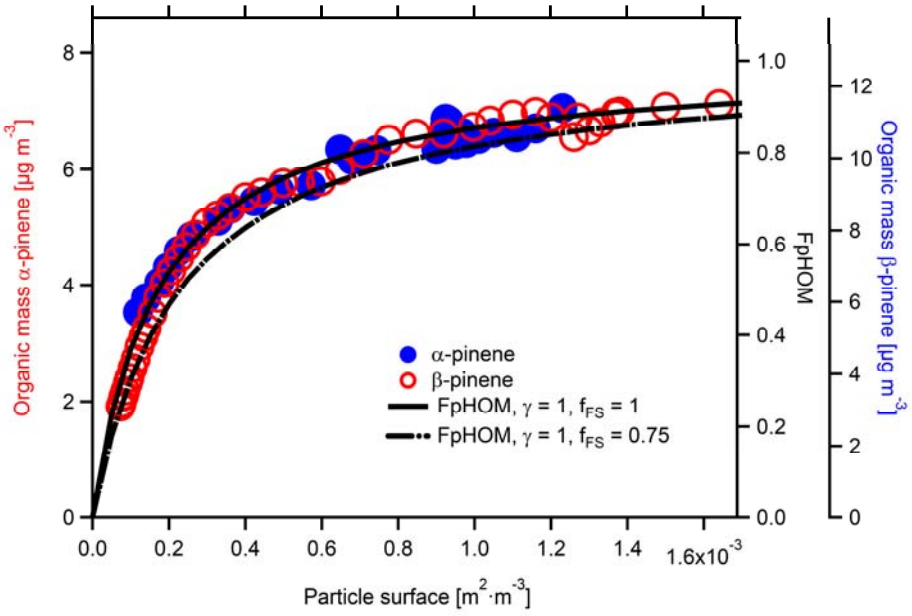

Figure S17: Organic mass as a function of increasing particle surface provided by seed particles. Production rates of HOM were held constant and seed particle concentrations were changed by flush out after stopping seed addition. If scaled, SOA formed by photooxidation of α-pinene at low NO_X (red open circles, left y-scale) and β-pinene at high NO_X (blue filled circles, right y-scale) show the same dependence on the particle surface. ([α-pinene]/[NOx] ~ 33 ppbC·ppb^{-1}), [β-pinene]/[NOx] ~ 1.8 ppbC·ppb^{-1}). The maximum load of ammonium sulfate seed particles was 88.5 µg m^{-3}; the number distribution was polydisperse, but monomodal with a mean diameter ~ 70 nm.
By definition Fp_{HOM} ranges from 0 to 1, and the axes were arranged for direct comparison with the measured data points. The black line shows Fp_{HOM} calculated for the HOM $C_{10}H_{16}O_7$ with molecular weight of 248 g/mol, $\bar{\upsilon}$ = 156 m s^{-1} for a wall loss rate = 0.0067 s^{-1} equivalent to a HOM lifetime of 150 s (compare Figure S16), uptake probability γ = 1, Fuchs-Sutugin factor f_{FS} = 1. The dashed dotted line shows that the effect of f_{FS} would be hardly detectable for $1>f_{FS}>0.75$ in Lp_{HOM}. For molecules with molecular formulas $C_{10}H_{16}O_{4\text{-}12}$ and 70 nm particles $f_{FS} > 0.85$ and neglection of f_{FS} causes only small effects.

If LVOC-HOM with substantial vapour pressures[39,72] are involved in SOA formation, the evaporation would manifest in such that Lw_{HOM} and Lp_{HOM} become net fluxes under our steady state conditions. This would simple become manifest in $\gamma < 1$. However, with the assumption of the same organic matrix on walls and particles, the γ cancel out and the same Fp also applies for LVOC-HOM. We therefore applied the correction Fp_{HOM} shown in Figure S17 to all our yield data.

Most experiments were performed at $S_{tot} > 6 \cdot 10^{-4}$ m^2 m^{-3}, i.e. the corrections applied were less than 30%. In some case with $S_{tot} < 0.4$ -0.1 $m^2 \cdot m^{-3}$ corrections from 1.5 to 2 were applied. A list of all applied correction factors is found in Table S1. The data were obtained at particle surface densities between $1.3 \cdot 10^{-4}$ to $1.9 \cdot 10^{-3}$ m^2 m^{-3}. This led to correction factors $1/Fp_{HOM}$ in the range between 1.1 and 2.4. The variation of $1/Fp_{HOM}$ was mainly caused by varying amounts of seed aerosol added during individual experimental runs. Within the experiment sets e.g. α-pinene alone (Table S1, top) or α-pinene&isoprene mixtures (Table S1, bottom), $1/Fp_{HOM}$ varied much less as the generation of seed particles by the atomizer was quite constant. Addition of isoprene to the α-pinene reaction system increased $1/Fp_{HOM}$ as the organic mass was reduced by the isoprene addition and therewith also the total particle surface. Removing isoprene from the reaction systems decreased $1/Fp_{HOM}$ because the organic mass and the size of the particles increased again. This shows that the net effect of isoprene, i.e. the OH scavenging effect and the product scavenging effect, would have been overestimated if the data would not have been corrected for the wall losses of the HOM.

However, due to the application of seed particles the changes in Fp_{HOM}, and thereby the changes in the correction factors were not very large. For the lowest particle surface used in these experiments, $1/Fp_{HOM}$ increased from 1.77 to 2.4 i.e. by roughly 35% due to the isoprene addition. In all other cases the values of $1/Fp_{HOM}$ increased by less than 16% when isoprene was added (see Table S1). We estimate the error caused by the correction procedure to ~20 % for the lowest particle surface and to ~10 % for the other data points[20]. Uncertainties in $1/Fp_{HOM}$ were therefore much lower than the effect of isoprene on mass formation.

Organic products deposited on the walls can also act as source for SOA, if they evaporate and condense onto the seed aerosols. This will happen when fresh seed aerosol is added to the chamber and perturbs the wall gas-phase equilibrium by condensation of gaseous components. We quantified potential transfer of SOA material from the walls to the seed aerosols by switching off the VOC source in the RC while keeping the oxidants O_3 or OH in place. The condensation of organic material of seed aerosols was monitored by AMS. (The results are partly positively biased by AMS, as AMS analysis a priori accounts unassigned signals to organics.)

During ozonolysis wall products generated 0.5 - 1.5 $\mu g/m^3$ SOA This contribution is relatively small (10% of maximum SOA) and stable, because products emerging from the walls cannot be further oxidized by ozone. If UV is turned on and OH is available, more SOA was produced on the seed aerosols as wall products can now be further oxidized leading to lower vapour pressure products. In the case of neutral ammonium sulfate the OH/wall product contribution after 60 h of

experiment was increased from 1.5 to 2.8 μg/m^3. [OH] was two times higher than in presence of α-pinene, which leads to an overestimation of the wall effect to the SOA mass observed during the core of the experiment.

The situation is different in the presence of acidic ammonium bisulfate aerosols. Here we measured 1.6 μg/m^3 of OH-wall contribution before the core experiment. The OH-wall contribution increased in the course of the experiment to about 4 μg/m^3 over 40 h. We attribute this increase to deposition of ammonium bisulfate particles which slowly acidified the walls and mobilized an increasing amount of acidic organic components. Again [OH] was 1.6 times higher than in the presence of α-pinene overestimating the true effect during the core experiments.

Note that the SOA baseline caused by wall deposits and their oxidation products will counteract the isoprene effect and makes our observations of the isoprene effects a lower limit. We therefore did not correct for the wall produced SOA, but subsumed the baseline effects under the error of our SOA yields.

10. References Supplement

45 Mentel, T. F. *et al.* Formation of highly oxidized multifunctional compounds: autoxidation of peroxy radicals formed in the ozonolysis of alkenes – deduced from structure–product relationships. *Atmos. Chem. Phys.* **15**, 6745-6765 (2015).

46 Mentel, T. F. *et al.* Photochemical production of aerosols from real plant emissions. *Atmos. Chem. Phys.* **9**, 4387-4406 (2009).

47 Heiden, A. C., Kobel, K., Langebartels, C., Schuh-Thomas, G. & Wildt, J. Emissions of oxygenated volatile organic compounds from plants - part I: Emissions from lipoxygenase activity. *J. Atmos. Chem.* **45**, 143-172 (2003).

48 Rubach, F. *Aerosol processes in the Planetary Boundary Layer: High resolution Aerosol Mass Spectrometry on a Zeppelin NT Airship*, Universität Wuppertal, (2013).

49 Mensah, A. A., Buchholz, A., Mentel, T. F., Tillmann, R. & Kiendler-Scharr, A. Aerosol mass spectrometric measurements of stable crystal hydrates of oxalates and inferred relative ionization efficiency of water. *J. Aerosol Sci.* **42**, 11-19 (2011).

50 Jimenez, J. L. *et al.* Comment on "The effects of molecular weight and thermal decomposition on the sensitivity of a thermal desorption aerosol mass spectrometer". *Aerosol Sci. Technol.* **50**, I-XV (2016).

51 Junninen, H. *et al.* A high-resolution mass spectrometer to measure atmospheric ion composition. *Atmos. Meas. Techn.* **3**, 1039-1053 (2010).

52 Ehn, M. *et al.* Gas phase formation of extremely oxidized pinene reaction products in chamber and ambient air. *Atmos. Chem. Phys.* **12**, 5113-5127 (2012).

53 Eisele, F. L. & Tanner, D. J. Measurement of the gas-phase concentration of H_2SO_4 and methane sulfonic acid and estimates of H_2SO_4 production and loss in the atmosphere. *J. Geophys. Res.-Atmos* **98**, 9001-9010 (1993).

54 Jokinen, T. *et al.* Atmospheric sulphuric acid and neutral cluster measurements using CI-APi-TOF. *Atmos. Chem. Phys.* **12**, 4117-4125 (2012).

55 Hyttinen, N., Rissanen, M. P. & Kurten, T. Computational Comparison of Acetate and Nitrate Chemical Ionization of Highly Oxidized Cyclohexene Ozonolysis Intermediates and Products. *J. Phys. Chem. A* **121**, 2172-2179 (2017).
56 Lindinger, W., Hansel, A. & Jordan, A. Proton-transfer-reaction mass spectrometry (PTR-MS): on-line monitoring of volatile organic compounds at pptv levels. *Chem. Soc. Rev.* **27**, 347-354 (1998).
57 Gautrois, M. & Koppmann, R. Diffusion technique for the production of gas standards for atmospheric measurements. *J. Chromatogr. A* **848**, 239-249 (1999).
58 Shrivastava, M. *et al.* Recent advances in understanding secondary organic aerosol: Implications for global climate forcing. *Rev. Geophys.* **55**, 509-559 (2017).
59 Rohrer, F. & Berresheim, H. Strong correlation between levels of tropospheric hydroxyl radicals and solar ultraviolet radiation. *Nature* **442**, 184-187 (2006).
60 Rohrer, F. *et al.* Maximum efficiency in the hydroxyl-radical-based self-cleansing of the troposphere. *Nature Geoscience* **7**, 559-563 (2014).
61 Donahue, N. M., Robinson, A. L., Stanier, C. O. & Pandis, S. N. Coupled partitioning, dilution, and chemical aging of semivolatile organics. *Environ. Sci. & Techn.* **40**, 2635-2643 (2006).
62 Pankow, J. F. An absorption model of gas-particle partitioning of organic compounds in the atmosphere. *Atmos. Environ.* **28**, 185-188 (1994).
63 Pankow, J. F. An absorption model of the gas aerosol partitioning involved in the formation of secondary organic aerosol. *Atmos. Environ.* **28**, 189-193 (1994).
64 van Donkelaar, A. *et al.* Model evidence for a significant source of secondary organic aerosol from isoprene. *Atmos. Environ.* **41**, 1267-1274 (2007).
65 Zhang, Y., Huang, J. P., Henze, D. K. & Seinfeld, J. H. Role of isoprene in secondary organic aerosol formation on a regional scale. *J. Geophys. Res.-Atmos* **112**, D20207 (2007).
66 D'Ambro, E. L. *et al.* Molecular composition and volatility of isoprene photochemical oxidation secondary organic aerosol under low- and high-NOx conditions. *Atmos. Chem. Phys.* **17**, 159-174 (2017).
67 Lin, Y. H. *et al.* Light-Absorbing Oligomer Formation in Secondary Organic Aerosol from Reactive Uptake of Isoprene Epoxydiols. *Environ. Sci. & Techn.* **48**, 12012-12021 (2014).
68 Lappalainen, H. K., *et al.*, Day-time concentrations of biogenic volatile organic compounds in a boreal forest canopy and their relation to environmental and biological factors. *Atmos. Chem. Phys*. **9**, 5447-5459 (2009).
69 Crounse, J. D., Paulot, F., Kjaergaard, H. G. & Wennberg, P. O. Peroxy radical isomerization in the oxidation of isoprene. *Physical Chemistry Chemical Physics* **13**, 13607-13613 (2011).
70 Rissanen, M. P. *et al.* The Formation of Highly Oxidized Multifunctional Products in the Ozonolysis of Cyclohexene. *J. Am. Chem. Soc.* **136**, 15596-15606 (2014).
71 Crounse, J. D., Nielsen, L. B., Jorgensen, S., Kjaergaard, H. G. & Wennberg, P. O. Autoxidation of Organic Compounds in the Atmosphere. *J. Phys. Chem. Lett.* **4**, 3513-3520 (2013).
72 Kurten, T. *et al.* Alpha-Pinene Autoxidation Products May Not Have Extremely Low Saturation Vapor Pressures Despite High O:C Ratios. *J. Phys. Chem. A* **120**, 2569-2582 (2016).

73 Chen, Q., Liu, Y. J., Donahue, N. M., Shilling, J. E. & Martin, S. T. Particle-Phase Chemistry of Secondary Organic Material: Modeled Compared to Measured O:C and H:C Elemental Ratios Provide Constraints. *Environ. Sci. & Techn.* **45**, 4763-4770, (2011).
74 D'Ambro, E. L. *et al.* Isomerization of Second-Generation Isoprene Peroxy Radicals: Epoxide Formation and Implications for Secondary Organic Aerosol Yields. *Environ. Sci. & Techn.* **51**, 4978-4987 (2017).
75 Kiendler-Scharr, A. *et al.* Isoprene in poplar emissions: effects on new particle formation and OH concentrations. *Atmos. Chem. Phys.* **12**, 1021-1030 (2012).
76 Krechmer, J. E. *et al.* Formation of Low Volatility Organic Compounds and Secondary Organic Aerosol from Isoprene Hydroxyhydroperoxide Low-NO Oxidation. *Environ. Sci. & Techn.* **49**, 10330-10339 (2015).
77 Kroll, J. H., Ng, N. L., Murphy, S. M., Flagan, R. C. & Seinfeld, J. H. Secondary organic aerosol formation from isoprene photooxidation. *Environ. Sci. & Techn.* **40**, 1869-1877, (2006).
78 Riva, M. *et al.* Chemical Characterization of Secondary Organic Aerosol from Oxidation of Isoprene Hydroxyhydroperoxides. *Environ. Sci. & Techn.* **50**, 9889-9899 (2016).
79 Berndt, T., Herrmann, H., Sipila, M. & Kulmala, M. Highly Oxidized Second-Generation Products from the Gas-Phase Reaction of OH Radicals with Isoprene. *J. Phys. Chem. A* **120**, 10150-10159 (2016).
80 Jenkin, M. E., Young, J. C. & Rickard, A. R. The MCM v3.3.1 degradation scheme for isoprene. *Atmos. Chem. Phys.* **15**, 11433-11459 (2015).
81 Peeters, J., Muller, J. F., Stavrakou, T. & Nguyen, V. S. Hydroxyl Radical Recycling in Isoprene Oxidation Driven by Hydrogen Bonding and Hydrogen Tunneling: The Upgraded LIM1 Mechanism. *J. Phys. Chem. A* **118**, 8625-8643 (2014).
82 Peeters, J., Nguyen, T. L. & Vereecken, L. HOx radical regeneration in the oxidation of isoprene. *Phys. Chem. Chem. Phys.* **11**, 5935-5939 (2009).
83 St Clair, J. M. *et al.* Kinetics and Products of the Reaction of the First-Generation Isoprene Hydroxy Hydroperoxide (ISOPOOH) with OH. *J. Phys. Chem. A* **120**, 1441-1451 (2016).
84 Brauers, T. & Rohrer, F. Brauers T. and Rohrer F., Easy AtmoSpheric Chemistry. Manual, Vers 2.9, http://www.fz-juelich.de/icg/icg-2/easy_doc, 1999.
85 Lin, Y. H. *et al.* Isoprene Epoxydiols as Precursors to Secondary Organic Aerosol Formation: Acid-Catalyzed Reactive Uptake Studies with Authentic Compounds. *Environ. Sci. & Techn.* **46**, 250-258 (2012).
86 Riedel, T. P. *et al.* Heterogeneous Reactions of Isoprene-Derived Epoxides: Reaction Probabilities and Molar Secondary Organic Aerosol Yield Estimates. *Environ. Sci. & Techn. Letters* **2**, 38-42 (2015).
87 Dommen, J. *et al.* Determination of the Aerosol Yield of Isoprene in the Presence of an Organic Seed with Carbon Isotope Analysis. *Environ. Sci. & Techn.* **43**, 6697-6702 (2009).
88 Wyche, K. P. *et al.* Emissions of biogenic volatile organic compounds and subsequent photochemical production of secondary organic aerosol in mesocosm studies of temperate and tropical plant species. *Atmos. Chem. Phys.* **14**, 12781-12801 (2014).
89 Simpson, D., Bergström, R., Imhof, H. & Wind, P. Updates to the EMEP/MSC-W model, 2016--2017 Transboundary particulate matter, photo-oxidants, acidifying and eutrophying components. Status Report 1/2017, The Norwegian Meteorological Institute, Oslo, Norway, www.emep.int, 115-122 (2017).

90 Watson, L. A., Shallcross, D. E., Utembe, S. R. & Jenkin, M. E. A Common Representative Intermediates (CRI) mechanism for VOC degradation. Part 2: Gas phase mechanism reduction. *Atmos. Environ.* **42**, 7196-7204 (2008).
91 Hodzic, A. *et al.* Rethinking the global secondary organic aerosol (SOA) budget: stronger production, faster removal, shorter lifetime. *Atmos. Chem. Phys.* **16**, 7917-7941 (2016).
92 Tsigaridis, K. *et al.* The AeroCom evaluation and intercomparison of organic aerosol in global models. *Atmos. Chem. Phys.* **14**, 10845-10895 (2014).
93 Arneth, A., Monson, R. K., Schurgers, G., Niinemets, U. & Palmer, P. I. Why are estimates of global terrestrial isoprene emissions so similar (and why is this not so for monoterpenes)? *Atmos. Chem. Phys.* **8**, 4605-4620 (2008).
94 Arneth, A., Schurgers, G., Hickler, T. & Miller, P. A. Effects of species composition, land surface cover, CO2 concentration and climate on isoprene emissions from European forests. *Plant Biol.* **10**, 150-162 (2008).
95 Bergström, R., van der Gon, H., Prevot, A. S. H., Yttri, K. E. & Simpson, D. Modelling of organic aerosols over Europe (2002-2007) using a volatility basis set (VBS) framework: application of different assumptions regarding the formation of secondary organic aerosol. *Atmos. Chem. Phys.* **12**, 8499-8527 (2012).
96 Messina, P. *et al.* Global biogenic volatile organic compound emissions in the ORCHIDEE and MEGAN models and sensitivity to key parameters. *Atmos. Chem. Phys.* **16**, 14169-14202 (2016).
97 Torseth, K. *et al.* Introduction to the European Monitoring and Evaluation Programme (EMEP) and observed atmospheric composition change during 1972-2009. *Atmos. Chem. Phys.* **12**, 5447-5481 (2012).
98 Solomon, P. A. *et al.* US National PM2.5 Chemical Speciation Monitoring Networks-CSN and IMPROVE: Description of networks. *J. Air Waste Manage* **64**, 1410-1438 (2014).
99 Wildt, J. *et al.* Suppression of new particle formation from monoterpene oxidation by NOx. *Atmos. Chem. Phys.* **14**, 2789-2804 (2014).
100 Anttila, T., Kiendler-Scharr, A., Tillmann, R. & Mentel, T. F. On the reactive uptake of gaseous compounds by organic-coated aqueous aerosols: Theoretical analysis and application to the heterogeneous hydrolysis of N_2O_5. *J. Phys. Chem. A* **110**, 10435-10443 (2006).
101 Fuchs, N. A., Sutugin, A. G., Hidy, G. M. & Brock, J. R. High-dispersed aerosols. *International Rev. of Aerosol Phys*. *Chem.* **2**, 1-60 (1971).
102 Fry, J. L. *et al.* Secondary Organic Aerosol Formation and Organic Nitrate Yield from NO_3 Oxidation of Biogenic Hydrocarbons. *Environ. Sci. & Techn.* **48**, 11944-11953 (2014).
103 Mentel, T. F. *et al.* Secondary aerosol formation from stress-induced biogenic emissions and possible climate feedbacks. *Atmos. Chem. Phys.* **13**, 8755-8770 (2013).